Published in final edited form as:
Surv Geophys. 2019 ; 40: 589–629. doi:10.1007/s10712-018-9478-y.

Quantifying Vegetation Biophysical Variables from Imaging Spectroscopy Data: A Review on Retrieval Methods

Jochem Verrelst[1], **Zbyněk Malenovský**[2,3,4], **Christiaan Van der Tol**[5], **Gustau Camps-Valls**[1], **Jean-Philippe Gastellu-Etchegorry**[6], **Philip Lewis**[7,8], **Peter North**[9], **Jose Moreno**[1]

[1]Image Processing Laboratory (IPL), Parc Científic, Universitat de València, Paterna, València 46980, Spain

[2]Surveying and Spatial Sciences Group, School of Technology, Environments and Design, University of Tasmania, Private Bag 76, Hobart, TAS 7001, Australia

[3]Remote Sensing Department, Global Change Research Institute CAS, Bělidla 986/4a, 60300 Brno, Czech Republic

[4]USRA/GESTAR, Biospheric Sciences Laboratory, NASA Goddard Space Flight Center, 8800 Greenbelt Rd, Greenbelt, MD 20771, USA

[5]Department of Water Resources, Faculty ITC, University of Twente, P.O. Box 217, 7500 AE Enschede, The Netherlands

[6]Centre d'Etudes Spatiales de la Biosphère - UPS, CNES, CNRS, IRD, Université de Toulouse, 31401 Toulouse Cedex 9, France

[7]Department of Geography, University College London, Pearson Building, Gower Street, WC1E 6BT London, UK

[8]National Centre for Earth Observation, Department of Physics and Astronomy, The University of Leicester, Michael Atiyah Building, LE1 7RH Leicester, UK

[9]Department of Geography, Swansea University, Swansea SA2 8PP, UK

Abstract

An unprecedented spectroscopic data stream will soon become available with forthcoming Earth-observing satellite missions equipped with imaging spectroradiometers. This data stream will open up a vast array of opportunities to quantify a diversity of biochemical and structural vegetation properties. The processing requirements for such large data streams require reliable retrieval techniques enabling the spatiotemporally explicit quantification of biophysical variables. With the aim of preparing for this new era of Earth observation, this review summarizes the state-of-the-art retrieval methods that have been applied in experimental imaging spectroscopy studies inferring all kinds of vegetation biophysical variables. Identified retrieval methods are categorized into: (1) parametric regression, including vegetation indices, shape indices and spectral transformations; (2) nonparametric regression, including linear and nonlinear machine learning regression algorithms;

Correspondence to: Jochem Verrelst.
✉Jochem Verrelst jochem.verrelst@uv.es.

Europe PMC Funders Author Manuscripts

(3) physically based, including inversion of radiative transfer models (RTMs) using numerical optimization and look-up table approaches; and (4) hybrid regression methods, which combine RTM simulations with machine learning regression methods. For each of these categories, an overview of widely applied methods with application to mapping vegetation properties is given. In view of processing imaging spectroscopy data, a critical aspect involves the challenge of dealing with spectral multicollinearity. The ability to provide robust estimates, retrieval uncertainties and acceptable retrieval processing speed are other important aspects in view of operational processing. Recommendations towards new-generation spectroscopy-based processing chains for operational production of biophysical variables are given.

Keywords

Imaging spectroscopy; Retrieval; Vegetation properties; Parametric and nonparametric regression; Machine learning; Radiative transfer models; Inversion; Uncertainties

1 Introduction

Quantitative vegetation variable extraction is fundamental to assess the dynamic response of vegetation to changing environmental conditions. Earth observation sensors in the optical domain enable the spatiotemporally explicit retrieval of plant biophysical variables. This data stream has never been so rich as is foreseen with the new-generation imaging spectrometer missions. The forthcoming EnMAP (Guanter et al. 2015), HyspIRI (Lee et al. 2015), PRISMA (Labate et al. 2009) and FLEX (Drusch et al. 2017) satellite missions will produce large spectroscopic data streams for land monitoring, which will soon become available to a diverse user community. This upcoming vast data stream will not only be standardized (e.g., atmospherically corrected), but will also require reliable and efficient retrieval processing techniques that are accurate, robust and fast.

Since the advent of optical remote sensing science, a variety of retrieval methods for vegetation attribute extraction emerged. Most of these methods have been applied to the data of traditional multispectral sensors (Verrelst et al. 2015), but increasingly they are also applied within imaging spectroscopy studies. This review provides a summary of recently developed methodologies to infer per-pixel biophysical variables from imaging spectroscopy data, covering the visible, near-infrared (NIR) and shortwave infrared spectral regions. Essentially, quantification of surface biophysical variables from spectral data always relies on a model, enabling the interpretation of spectral observations and their translation into a surface biophysical variable. Biophysical variable retrievals, as traditionally described in the terrestrial remote sensing literature, are grouped into two categories: (1) the statistical (or variable-driven) category and (2) the physical (or radiometric data-driven) category (Baret and Buis 2008). Over the last decade, however, both methodological categories expanded into subcategories and combinations thereof. Exemplary is the increasing number of elements of both categories which have been integrated into *hybrid* approaches. This methodological expansion, therefore, demands for a more systematic categorization. From an optical remote sensing point of view, and in line with an earlier, more general review

Europe PMC Funders Author Manuscripts

paper (Verrelst et al. 2015), retrieval methods can be classified in the following four methodological categories:

1. *Parametric regression methods* Parametric methods assume an explicit relationship between spectral observations and a specific biophysical variable. Thus, explicit parameterized expressions are built; they are usually based on some physical knowledge of absorption and scattering properties and statistical relationship between the variable and the spectral response. Typically, a band arithmetic formulation is defined (e.g., a spectral index) and then linked to the variable of interest based on a fitting function.

2. *Nonparametric regression methods* Nonparametric methods directly define regression functions according to information from the given spectral data and associated variable, i.e. they are data-driven methods. Hence, in contrast to parametric regression methods, a non-explicit choice is to be made on spectral band relationships, transformation(s) or fitting function. Nonparametric methods can further be split into linear or nonlinear regression methods.

3. *Physically based model inversion methods* Physically based algorithms are applications of physical laws establishing photon interaction cause–effect relationships. Model variables are inferred based on specific knowledge, typically obtained with radiative transfer functions.

4. *Hybrid regression methods* A hybrid-method combines elements of nonparametric statistics and physically based methods. Hybrid models rely on the generic properties of physically based methods combined with the flexibility and computational efficiency of nonparametric nonlinear regression methods.

These categories provide a theoretical framework to organize the myriad of retrieval methods, as well to overview the diversity of published imaging spectroscopy applications based on these methods. However, a few remarks must be considered. One should be aware that the boundaries of these categories are not always clearly defined; for instance, spectral indices are also often used as input into nonparametric methods. Another important aspect is that the majority of the methods reviewed here is not exclusively designed for retrieval of biophysical variables. This especially holds for the statistical methods, whereby a regression model is used to link spectral data with a biophysical variable. In optical remote sensing science, these methods are commonly applied to map any feasible continuous variable, as well in the domains of snow, water or soil properties [see Matthews (2011), Mulder et al. (2011) and Dietz et al. (2012) for reviews]. Nevertheless, to keep this review comprehensive, it is limited to retrieval methods with applications in the domain of vegetation properties mapping. On the other hand, even within these boundaries each of the above methodological categories continues to be expanded with all kinds of spectroscopic data processing applications (e.g., Gewali et al. 2018). The drivers behind this methodological expansion can be found in the: (1) the interminable increase in computational power, (2) the increasing availability and democratizing of spectroscopic data, and (3) the steady progress in imaging spectroscopy sensor technology, which produces each time more sensitive sensors. This progress in imaging spectroscopy technology enables us to infer each time more subtle and highly dynamic vegetation properties from spectral data. For instance, the forthcoming

Europe PMC Funders Author Manuscripts

FLEX mission aims to deliver a portfolio of dynamic plant stress and productivity variables based on, among others, the exploitation of sun-induced chlorophyll fluorescence emitted by terrestrial vegetation (Drusch et al. 2017). Hence, this underlines the fact that the list of biophysical variables that can be extracted from imaging spectroscopy is not closed, but instead continues to grow with ongoing progress in spectrometer technology. Consequently, biophysical variables are in this review paper defined as any vegetation property that can be quantified, i.e. any pigments, chemical constituents, structural variables, but also variables related to plant photosynthesis, productivity or diseases. Altogether, the drivers behind methodological expansion are not mutually exclusive, but they strengthen each other, which leads to a rapid progress in the development of advanced retrieval methods that goes hand in hand with improved capabilities to quantify a broad diversity of biophysical variables. As will be demonstrated throughout this review, these trends are resulting in an unprecedented richness of imaging spectroscopy mapping applications.

Regardless of the methodology used or the targeted application, the principal characteristic of spectroscopic data lies in their dense information content embedded in a few hundred spectrally narrow bands. Although such a spectrally dense data source proved to be beneficial for the majority of targeted mapping applications, a key challenge for many retrieval methods is how to deal with spectral multicollinearity, i.e. band redundancy. Special attention, therefore, will be devoted to address common spectroscopic data processing challenges, and solutions will be given how to overcome them. Finally, while imaging spectrometers are so far mostly applied in an experimental context, the developments towards operational systems have manifestly taken off and undoubtedly will lead to new directions and possibilities of Earth observation. In view of getting prepared for these upcoming global spectroscopic data streams, we will close this review with recommendations about the possibilities of integrating promising retrieval approaches into operational schemes.

2 Parametric Regression Methods

Parametric regression methods have long been the most popular method to quantify biophysical variables in optical remote sensing, and the field of imaging spectroscopy is no exception to that. This simplest way of developing a regression model explicitly determines parameterized expressions relating a limited number of spectral bands with a biophysical variable of interest. The empirical models rely on a selection of bands with high sensitivity towards the variable of interest, typically in combination with subtle spectral features to reduce undesired effects, related to variations of, for instance, other leaf or canopy properties, background soil reflectance, solar illumination and sensor viewing geometry and atmospheric composition (e.g., Verrelst et al. 2008, 2010). In the following overview, we present common parametric regression methods, which are based on (1) vegetation indices, (2) shape indices and (3) spectral transformations (Fig. 1).

2.1 Discrete Spectral Band Approaches: Vegetation Indices

Parametric regression models based on vegetation indices (VIs) are by far the oldest and largest group of variable estimation approaches. VIs are defined to enhance spectral

features sensitive to a vegetation property, while reducing disturbances by combining some spectral bands into a VI (Clevers 2014; Glenn et al. 2008). The main advantage of VIs is their intrinsic simplicity. VI-based methods found their origin in the first applications of broadband sensor satellites. During the pioneering years of optical remote sensing, only a small set of spectral bands were available and computational power was limited. It led to a long tradition of the development of simple two bands, or at most three to four band indices that continues until today (e.g., Kira et al. 2016). New possibilities have opened with the advent of imaging spectrometers. Optimized narrowband information extraction algorithms were developed based on adaptations of established index formulations, such as simple ratio and normalized difference [see reviews by Clevers (2014), Glenn et al. (2008), Xue and Su (2017)]. On the other hand, the possibilities to develop spectral indices based on a few band combinations grew exponentially, and that demanded more systematic band evaluation methods.

A popular solution involves correlating all possible band combinations according to established index formulations. For two-band index formulations, such as simple ratio or normalized difference, this approach leads to 2D correlation matrices, which enables to visually identify optimal band combinations (e.g., Atzberger et al. 2010; Maire et al. 2004, 2008; Mariotto et al. 2013; Rivera et al. 2014; Thenkabail et al. 2000). Subsequently, given all possible combinations permit to select a ‘best-performing index’. Nevertheless, while being mathematically simple, this method is not only tedious—especially when evaluating all possible combinations of more than two bands—but also keeps on being restricted to formulations that make use of a few bands only, with at most using three or four bands. Thus, although the approach is systematic, it continues to underexploit the comprehensive information content hidden in the contiguous spectral data. Moreover, when applying this technique in mapping applications making use of imaging spectroscopy, identical best-performing spectral band combinations for the same biophysical variable have rarely been reported. This suggests that optimized narrowband VIs are strongly case specific and seem to lack generic capacity (Gonsamo 2011; Heiskanen et al. 2013; Mariotto et al. 2013).

More fundamentally, it remains dubious whether relying on transformed data originating from a few discrete bands fully captures the complexity of real-world observation conditions as has been observed by a spectroradiometer. Reducing full-spectrum datasets into simple indices formulations intrinsically leads to remaining spectral information left unexploited. Accordingly, the following two aspects should be considered to ensure optimized use of VIs in a spectroscopic context: (1) *Band selection*. Spectral indices are mathematical functions based on discrete bands, or at best a subset of full spectral information. Thus, the question arises: how do we assess with high enough accuracy whether the most sensitive spectral bands—with respect to biophysical variable retrieval—have been selected? (2) *Formulation*. Enhancing spectral information according to a mathematical transformation should lead to an optimal sensitivity of the spectral signal with respect to the variable of interest. While established formulations such as the simple ratio or normalized difference are commonly used, here the question arises again: how can we be sure whether these linear formulations are the most powerful ones with respect to biophysical variable retrieval? These two questions are almost impossible to resolve considering the unlimited possibilities of band

selections together with designing index formulations. Consequently, given their inherent constraints, it can be concluded that VI-based regression models exploit spectroscopic data suboptimally.

2.2 Parametric Approaches Based on Spectral Shapes and Spectral Transformations

Because none of the above few band index methods take full advantage of spectroscopic datasets, alternative methods were pursued with the advent of hyperspectral spectroradiometers that allow us to exploit specific absorption regions of the reflectance spectrum. It led to the development of so-called *shape* indices and spectral transformation methods. Shape indices, listed below, extract shape-related information from contiguous spectral signatures for a specific spectral region that is then correlated with a biophysical variable. These types of parametric methods are therefore exclusively applicable to spectroscopic data. The following categories can be identified:

- *Red-edge position (REP) calculations*. Mathematically, the REP inflection point is the position of a wavelength defined as the maximum of the first derivative reflectance between the red and NIR regions, i.e. between 670 and 780 nm (Kanke et al. 2016). The red-edge position is known to be sensitive to multiple biophysical variable variations, both chlorophyll pigments (Delegido et al. 2011) and structural variables, for instance the leaf area index (LAI) (Delegido et al. 2013). Therefore, REP-related methods are typically used to derive canopy chlorophyll content, being the product of LAI and leaf chlorophyll content (Clevers and Kooistra 2012; Li et al. 2017). Many mathematical approaches have been proposed to exploit this region as a sensitive indicator, including: (1) high-order curve fitting (Broge and Leblanc 2001; Clevers et al. 2004; (2) inverted Gaussian models (Cho and Skidmore 2006; Cho et al. 2008; Miller et al. 1990; (3) linear interpolation and extrapolation methods (Cho et al. 2008; Tian et al. 2011; 4) Lagrangian interpolation (Dawson et al. 1998; Pu et al. 2003; (5) rational function application (Baranoski and Rokne 2005); and, more recently, (6) a wavelet-based technique (Li et al. 2017).
- *Derivative-based indices*. Although several of the above-described methods make use of derivatives, e.g., linear extrapolation (Cho and Skidmore 2006) and Lagrangian technique (Dawson et al. 1998), the calculation of a derivative does not have to be restricted to the red edge. The derivative of any spectral region can be calculated and transformed into an index (Elvidge and Chen 1995; Penuelas et al. 1994; Sims and Gamon 2002; Zarco-Tejada et al. 2002). A systematic comparison of first derivative-based indices and conventional indices was performed by Maire et al. (2004) using the leaf optical model PROSPECT. Interestingly, the authors concluded that derivative-based indices are not necessarily better than conventional and properly elaborated indices.
- *Integration-based indices*. Alternatively, some authors proposed to calculate finite integrals of specific spectral regions, typically covering a part of the visible and the red-edge region for LAI or chlorophyll content estimations, into a (normalized) index (Broge and Leblanc 2001; Delegido et al. 2010; Malenovský et al. 2006, 2015; Mutanga et al. 2005; Oppelt and Mauser 2004). Likewise,

Europe PMC Funders Author Manuscripts

in a recent study of Pasqualotto et al. (2018) this method exploited the water absorption spectral regions to quantify canopy water content. In these studies, integration-based indices were demonstrated to perform superior to classical vegetation indices, as they exploit more optimally absorption regions embedded in spectroscopic data than indices relying on a reflectance intensity of few individual bands (Kováč et al. 2013). It can be expected that with the upcoming free availability of imaging spectroscopy data more methods of this kind of that explicitly exploit absorption features related to foliar constituents and pigments will emerge.

- *Continuum removal*. Whereas the above techniques focus on one or more specific spectral regions, continuum removal is a spectral transformation that can be applied over the full spectrum. This technique normalizes reflectance spectra, allowing comparison of individual absorption features with a common baseline (Clark and Roush 1984). The continuum removal transformation enhances and standardizes the specific absorption features related to vegetation properties. Continuum removal can be considered as a standard spectroscopic data processing technique and has found its way into various image processing software packages. Spectroscopic examples of applications include mapping of chlorophyll (Broge and Leblanc 2001; Malenovský et al. 2013, 2017), numerous studies on mapping nitrogen content (Huang et al. 2004; Mitchell et al. 2012; Mutanga and Kumar 2007; Mutanga and Skidmore 2004; Schlerf et al. 2010; Yao et al. 2015), foliar water condition (Stimson et al. 2005), plant stress (Sanches et al. 2014) and grassland biomass (Buchhorn et al. 2013; Cho et al. 2007).
- *Wavelet transform*. Wavelet analysis has been increasingly used to extract information from spectral data, e.g., related to vegetation properties (Rivard et al. 2008). Processing of reflectance spectra with wavelets can be performed as discrete or continuous (CWT) transforms. CWT outputs are directly comparable to the original spectrum and are simple to interpret. In this case, the original spectrum is represented by a set of spectra from small (narrow bandwidth absorption feature and noise) to larger scales (broad features, continuum). By selecting small-scale spectra (i.e. discarding the smallest scale, which contains white noise and high scales related to the continuum), the absorption features of the components are enhanced, preserving the spectral information of the original data (Scafutto et al. 2016). Based on the type of wavelet transform, specific bands sensitive to the targeted variable are then selected (Bao et al. 2017). CWT is often compared in spectroscopic studies against spectral indices and was found to be capable of delivering stronger correlations, e.g., in the detection of wheat aphid pests (Luo et al. 2013), LAI estimation (Huang et al. 2014), nitrogen content and chlorophyll content estimation (He et al. 2015; Kalacska et al. 2015; Luo et al. 2013) and in amplifying spectral separability of alpine wetland grass species (Bao et al. 2017).

Altogether, correlations based on shape indices and spectral transformations are undoubtedly more sophisticated normalization approaches than traditional spectral indices for exploiting

the spectral information embedded in spectroscopic data. Moreover, their relatively simple mathematical formulation ensures fast processing. It thus seems logical that these spectral transformation methods became standard spectroscopy image processing techniques. However, these methods alone provide nothing more than spectral transformations and enhancements. When aiming to estimate a biophysical variable, a fitting function—typically a linear least squares fitting, but also exponential, power and polynomial— is still required. Yet it remains questionable whether the selected fitting function is the most suitable one. Moreover, since parametric approaches are based on relatively simple mathematical definitions—as opposed to more advanced methods—no associated uncertainty intervals are provided. Although their strengths lie in their straightforward use and fast processing, with the absence of a per-pixel uncertainty estimate, the performance quality of parametric regression methods as a mapping method is hard to judge. Given the surface diversity captured in a single airborne or spaceborne image, and despite a standard validation exercise for a number of pixels, it still remains unknown how the retrieval quality evolves throughout a complete image. The absence of a quality indicator is, therefore, in our view the main reason why parametric regression methods (Fig. 2) are not recommendable for operational quantification of biophysical variables.

3 Nonparametric Regression Methods

Contrary to parametric methods, nonparametric methods optimize the regression algorithm by means of an inherent learning phase based on training data. Essentially, the nonparametric model develops weights (coefficients) adjusted to minimize the estimation error of the variables extracted. This means that no explicit parametrization is required, which practically simplifies the model development, but more expert knowledge to understand and execute these models may be required. Another important advantage of nonparametric methods is the possibility of training with the full-spectrum information. Hence, an explicit selection of spectral bands or transformations is in principle not required. A flexible model is able to combine different data structure features in a nonlinear manner to conform requirements; however, model definition with a too flexible capacity may incur the problem of overfitting the training dataset. To avoid this pitfall, model weights are defined by jointly minimizing the training set approximation error while limiting the model complexity. In view of processing spectroscopic data, a more prevalent problem lies in the so-called *curse of dimensionality* (Hughes phenomenon) (Hughes 1968). Adjacent, contiguous bands carry highly intercorrelated information, which may result in redundant data and possible noise and potentially suboptimal regression performances. As discussed further on, band selection or dimensionality reduction methods that transform the spectral data to lower-dimensional space, while containing the vast majority of the original information, can overcome this problem (Fig. 3).

3.1 Linear Nonparametric Methods

Nonparametric regression algorithms that apply linear transformations are attractive because of their fast performance. These methods became standard methods in chemometric and in image processing software packages. Multivariable linear regression methods can cope with spectroscopic data and typically rely on the estimation of co-variances. When moving

towards spectroscopic data, however, this can become problematic when input data quantity is limited with respect to the dimensionality of the dataset. To alleviate collinearity, often linear nonparametric methods are applied in combination with a dimensionality reduction step. Some methods are even intrinsically based on this principle, i.e. principal component regression (PCR) (Wold et al. 1987) and partial least squares regression (PLSR) (Geladi and Kowalski 1986). Common linear nonparametric regression approaches are provided in Table 1, and imaging spectroscopy applications are discussed below.

On the application side, stepwise multiple linear regression (SMLR) is a classical multivariable regression algorithm commonly applied in chemometrics (Atzberger et al. 2010). To evaluate its predictive power, SMLR has been often compared with alternative regression techniques such as PLSR and some studies concluded that PLSR yielded better results when estimating LAI (Darvishzadeh et al. 2008) and canopy chlorophyll content (Atzberger et al. 2010). Also Ramoelo et al. (2011) compared both regression algorithms to estimate foliar nitrogen and phosphorus in combination with continuum removal using field spectrometry. By estimating canopy nitrogen, Miphokasap et al. (2012) demonstrated that the model developed by SMLR led to a higher correlation coefficient and lower errors than model applications based on narrowband VIs. This suggests that nonparametric (full-spectrum) models tend to be more powerful than parametric models. Likewise, Yi et al. (2014) compared SMLR with PLSR and spectral indices for carotenoid estimation in cotton and concluded that best estimations were obtained with PLSR. Likewise, SMLR was compared with PLSR and (nonlinear) machine learning regression algorithms for estimating leaf nitrogen content (Yao et al. 2015). Because of their enhanced flexibility, it may not be a surprise that the nonlinear methods outperformed SMLR and PLSR. This was also observed by various similar studies, as will be addressed in Sect. 3.2.

PCR seems to be more effective in the conversion of spectroscopic data into the estimation of vegetation properties, because the PCA-based dimensionality reduction method is embedded in the method in combination with a linear regression function. Hence, by converting the spectral data to a lower-dimensional space automatically overcomes the band redundancy problem. This method has been improved with PLSR, where the projections are optimized in view of the regression. It is, therefore, not a surprise that only few spectroscopic studies examined the predictive power of PCR. Those studies compared PCR against PLSR or against VIs (Atzberger et al. 2010; Fu et al. 2012; Marshall and Thenka-bail 2014; Rivera Caicedo et al. 2014; Wang et al. 2017b). Although PCR generally out-performed VIs in explaining variability of a vegetation attribute, in all cases PLSR or any other nonparametric method overran PCR.

PLSR found its way into a broad diversity of imaging spectroscopy applications, especially in the mapping of biochemicals, pigments and vegetation density properties. For instance, PLSR was used in several spectroscopic studies applied to estimate foliage nitrogen content (Coops et al. 2003; Hansen and Schjoerring 2003; Huang et al. 2004). Also Gianelle and Fb (2007) used PLSR to derive grassland phytomass and its total (percentage) nitrogen content from spectroscopic data. Similarly, Cho et al. (2007) and Im et al. (2009) applied PLSR to estimate a diversity of grass and crop biophysical variables (LAI, stem biomass and leaf nutrient concentrations), and Ye et al. (2007) applied PLSR for yield prediction purposes.

Beyond individual vegetation attributes, PLSR was recently used to predict landscape-scale fluxes of net ecosystem exchange (NEE) and gross primary productivity (GPP) across multiple timescales (Matthes et al. 2015), and also for the estimation of floristic composition of grassland ecosystems (Harris et al. 2015; Neumann et al. 2016; Roth et al. 2015). At the same time, thanks to its PLS-vectors, PLSR is also increasingly applied for band sensitivity analysis of spectroscopic datasets in view of the targeted application (e.g., Feilhauer et al. 2015; Kiala et al. 2016; Kira et al. 2016; Li et al. 2014a; Neumann et al. 2016). Various experimental studies demonstrated the superior predictive power of PLSR as opposed to VIs for the prediction of multiple vegetation properties, including above-ground biomass, LAI, leaf pigments (chlorophyll, carotenoids), GPP and NEE fluxes, leaf rust disease detection and nutrients concentration (nitrogen and phosphorus concentrations) (Capolupo et al. 2015; Dreccer et al. 2014; Foster et al. 2017; Hansen and Schjoerring 2003; Matthes et al. 2015; Wang et al. 2017a; Yue et al. 2017). However, when compared against machine learning methods, then PLSR no longer appeared to be top performing (Ashourloo et al. 2016; Kiala et al. 2016; Wang et al. 2015; Yao et al. 2015). As will be addressed in Sect. 3.2, this is due to the nonlinear transformation conducted in machine learning methods.

Other linear nonparametric regression methods, such as ridge regression (RR) and LASSO, hardly made it into applications for vegetation properties mapping. Yet a few spectroscopic examples are worth mentioning. For instance, Addink et al. (2007) used RR to map LAI and biomass, and more recently Bratsch et al. (2017) applied LASSO to estimate above-ground biomass quantities among different plant tissue type categories in Alaska. In another biomass estimation study, both RR and LASSO were compared against PLSR (Lazaridis et al. 2010) and also random forests (Zandler et al. 2015). Interestingly, RR and LASSO appeared to be top performing. One may, therefore, wonder why these techniques have not been applied more often. On the other hand, these linear methods are increasingly replaced by their nonlinear counterparts. For instance, RR has been replaced by kernel ridge regression (KRR) (Suykens and Vandewalle 1999), and also PLSR has been redesigned into a kernel version, i.e. the KPLSR, which proved to be more powerful than PLSR for chlorophyll concentration estimation (Arenas-García and Camps-Valls 2008). The family of kernel methods is addressed in Sect. 3.2. That none of these linear nonparametric methods (Fig. 4) deliver uncertainty estimates is another drawback. Similar as in case of parametric regression, without uncertainty estimates it remains questionable whether these methods can deliver consistent mapping quality throughout a complete image, or are applicable to other images in space and time.

3.2 Nonlinear Nonparametric Methods

When advancing beyond linear transformation techniques, a diversity of nonlinear non-parametric methods has been developed during last few decades. These methods, also referred to as machine learning regression algorithms, apply nonlinear transformations. An important methodological advantage is their capability to capture nonlinear relationships of image features without explicitly knowing the underlying data distribution. Hence, they are developed without assuming a particular probability density distribution, which is the reason why they work well with all kinds of data types. Machine learning methods also offer the possibility to incorporate a prior knowledge and the flexibility to include different data types

into the analysis. In principle, they are perfectly suited to process spectroscopic data. In the following sections, examples of the families of (1) decision trees, (2) artificial neural networks and (3) kernel-based regression are explained.

3.2.1 Decision Trees—Decision tree algorithms use a branching method to illustrate every possible outcome of a decision (Table 2). They are more frequently applied in classification than in regression. Only a few decision tree feasibility studies dealing with imaging spectroscopy data are presented in the scientific literature (e.g., Im et al. 2009) most likely because boosted and bagging trees hardly found their way to regression applications. They might be considered as obsolete with the improvements introduced into random forest (RF), which is essentially a specific type of bagging trees. RF builds an ensemble of individual decision trees working with different subsets of features (bands) and eventually different training data points both selected randomly, from which a final prediction is made using particular combination schemes. RF can handle a large number of training samples, does not suffer from overfitting and is robust to outliers and noise (Belgiu and Drăguţ 2016), which makes it an attractive method for spectroscopic mapping applications. RF has recently been made available in various software packages and proved to be a competent regression algorithm. It therefore comes as no surprise that RF gained rapid popularity in imaging spectroscopy mapping of a diverse range of vegetation attributes, including biomass (Adam et al. 2014; Vaglio Laurin et al. 2014), canopy nitrogen (Li et al. 2014) and as indicator of plant species composition (Feilhauer et al. 2017). Some of these studies have compared RF with support vector regression (SVR) or neural networks, but no strong preference towards one or the other method was found, which suggests that all three methods are competitive (Han et al. 2016; Pullanagari et al. 2016). However, just like other machine learning regression methods, RF can face difficulties coping with the collinearity of the spectroscopic data (Rivera-Caicedo et al. 2017). To overcome this problem, RF is often used in combination with sensitive bands or simple transformations in the form of VIs that are known to be sensitive to the targeted vegetation property (Adam et al. 2014; Han et al. 2016; Liang et al. 2016). Alternatively, RF is inherently able to identify sensitive spectral bands, and selection of only those sensitive bands can subsequently improve the regression model (Balzarolo et al. 2015; Feilhauer et al. 2015). Whether applying a band selection method is the most successful strategy, however, remains an open question. Rather than seeking for optimized individual bands, a more elegant solution may lie in firstly applying dimensionality reduction method and then inputting the features of the lower-dimensional space (i.e. components) into the decision tree (Rivera-Caicedo et al. 2017).

3.2.2 Artificial Neural Networks—Artificial neural network (ANN) methods are listed in Table 3. Since the early 1990s, feed-forward and back-propagation ANNs thrived in all kinds of mapping applications, including vegetation properties mapping (Francl and Panigrahi 1997; Kimes et al. 1998; Paruelo and Tomasel 1997). Their strengths lie in their adaptability that can lead to excellent performances. The superiority of ANNs in vegetation properties mapping compared to parametric models (e.g., those based on VIs) has been demonstrated repeatedly in experimental studies (Kalacska et al. 2015; Malenovský et al. 2013; Uno et al. 2005; Wang et al. 2013). Examples of successful spectroscopic applications include the estimation of foliage nitrogen concentrations (Huang et al. 2004)

and LAI (Jensen et al. 2012; Neinavaz et al. 2016). In both cited studies, ANN outperformed other linear nonparametric models (e.g., PLSR). Alternative powerful structures involve RBFANNs, BRANNs and RANNs (for explanation, see Table 3). Although these advanced ANNs have been primarily used for classification applications, only recently they were explored to map vegetation properties from spectroscopic data (Chen et al. 2015; Feng et al. 2016; Pôças et al. 2017; Wang et al. 2013). Some of these studies mention the superiority of these advanced ANN designs as compared to standard ANN designs or other machine learning approaches in estimating vegetation properties (Du et al. 2016; Li et al. 2017; Pham et al. 2017).

Applying ANNs to spectroscopic data, nonetheless, can be quite challenging due to the multicollinearity. Feeding many bands into an ANN requires a complex design and consequently a long training time. Just as with decision trees, a popular approach is applying a band selection or the calculation of several sensitive VIs or shape indices such as red-edge position that are then entered either individually or as a combination into the ANN. Various of these band selection studies investigated combinations of VIs that led to the best prediction models (Chen et al. 2015; Feng et al. 2016; Jia et al. 2013; Liang et al. 2015; Mutanga and Kumar 2007; Pôças et al. 2017; Schlerf and Atzberger 2006). As discussed before, it remains questionable whether the selected indices preserve a maximum amount of useful information. On the contrary, when compressing the spectral data using dimensionality reduction methods into a lower-dimensional space, then it is ensured that a maximum amount of spectral information is preserved. This approach was applied, e.g., to assess corn yield (Uno et al. 2005) and phosphorus and nitrogen concentrations (Knox et al. 2011).

It is therefore not surprising that a study comparing PCA vs. indices inputted into ANNs concluded that the PCA-ANN design outperformed VI-ANN designs (Liu and Pan 2017). Moreover, given that only linear transformations are applied in PCA, it may even be that more adaptive dimensionality reduction methods yield superior accuracies when combined with ANN, e.g., partial least squares (PLS), or in the field of nonlinear kernel-based dimensionality reduction methods, e.g., kernel PCA (KPCA) or kernel PLS (KPLS). To ascertain this hypothesis, PCA was compared against 10 alternative dimensionality reduction methods in combination with ANN to carry out LAI estimation. As expected, various alternative dimensionality reduction methods outperformed PCA in developing accurate models (e.g., PLS, KPLS, KPCA) (Rivera-Caicedo et al. 2017).

3.2.3 Kernel-Based Machine Learning Regression Methods—Kernel-based regression methods solve nonlinear regression problems by transferring the data to a higher-dimensional space by a kernel function (Table 4). The flexibility offered by kernel methods allows us to transform almost any linear algorithm that can be expressed in terms of dot products, while still using only linear algebra operations. Kernel methods provide a consistent theoretical framework for developing nonlinear techniques and have useful properties when dealing with a low number of (potentially high-dimensional) training samples, and outliers and noise in the data (Gómez-Chova et al. 2011; Tuia et al. 2018). Given these attractive properties, kernel-based regression methods seem perfectly suited to extract nonlinear information related to vegetation properties from imaging spectroscopy

data. Developed in the mid-1990s, among the most popular kernel-based method for classification purposes involves SVM. Its regression version (SVR) gained popularity for the retrieval of continuous vegetation attributes from imaging spectroscopy data in the last decade. Examples include plant height, leaf nitrogen content and leaf chlorophyll content (Karimi et al. 2008; Yang et al. 2011). A multi-output version of SVR was presented by Tuia et al. (2011), with LAI, leaf chlorophyll content and fractional vegetation content being simultaneously estimated. Recently, SVR was used for processing spectroscopic images of sub-decimetre spatial resolution as acquired by low-altitude unmanned aircraft system to infer Antarctic moss vigour (Malenovský et al. 2017). Yet just as with the other advanced regression methods, SVR faces the same difficulties of coping with multicollinearity. Therefore, SVR has been commonly applied in combination with specific spectral subsets or VIs (Lin et al. 2013; Marabel and Alvarez-Taboada 2013), or with wavelet transforms (He et al. 2015). To deal with spectroscopic band redundancy, an advantage of SVR is that it allows band selection (analogous as PLSR and RF), which in principle allows the development of more optimized models (Feilhauer et al. 2015). On the other hand, it is likely that the combination with dimensionality reduction methods will lead to more powerful models (Rivera-Caicedo et al. 2017). To assess its predictive power, various spectroscopic studies compared SVR against similar methods such as SMLR or PLSR, although some band selection method appeared to be essential (Kiala et al. 2016; Wang et al. 2015; Yao et al. 2015). Conversely, when comparing SVR against other machine learning methods such as RF or GPR, then SVR no longer excelled (Pullanagari et al. 2016).

Kernel ridge regression (KRR) emerged as one of the promising upcoming kernel-based regression methods, although only a few spectroscopic studies have used it. For instance, Wang et al. (2011) compared KRR with linear nonparametric methods (multiple linear regression and PLSR) for LAI estimation. The authors concluded that KRR yielded the most accurate estimates. Also Peng et al. (2011) used KRR for the detection of chlorophyll content. Apart from these two studies, the spectroscopy vegetation community may not yet be familiar with this method. Solely Rivera Caicedo et al. (2014) had compared KRR against other machine learning algorithms applied to CHRIS (62 bands) and HyMap (125 bands) spectroscopic data for LAI mapping. In that study, KRR not only proved to be a very competitive regression algorithm, but also proved to be extremely fast. This is due to its relatively simple design that requires only one hyperparameter to be tuned. Because of its simplicity, another advantage is that KRR is capable of dealing with collinearity; the method can cope with thousands of contiguous bands. In fact, in the dimensionality reduction comparison study tested with simulated (2100 bands) and HyMap data (Rivera-Caicedo et al. 2017), KRR was the only regression method where dimensionality reduction methods did not lead to improvements as compared to using all bands. In conclusion, KRR emerged as an attractive regression method due to its competitive performance, fast processing and ease of dealing with spectroscopic data.

From all machine learning regression algorithms, probably the most exciting one is Gaussian process regression (GPR). Contrary to other methods, the training phase in GPR takes place in a Bayesian framework, leading to probabilistic outputs (Camps-Valls et al. 2016; Rasmussen and Williams 2006). GPR applied to spectroscopic data started only recently, e.g., for airborne HyMap mapping of leaf chlorophyll content (Verrelst et al. 2013a), and

for spaceborne CHRIS mapping of leaf chlorophyll content, LAI and fractional vegetation content (Verrelst et al. 2012a). Of interest is that along with these maps also maps of associated uncertainties (prediction intervals) were provided. Also with an Airborne Hyperspectral Scanner, Roelofsen et al. (2014) applied GPR to map salinity, moisture and nutrient concentrations that in turn were used as inputs for plant association mapping. In the Rivera Caicedo et al. (2014) comparison paper, GPR outperformed the majority of other tested machine learning methods for the prediction of leaf chlorophyll content and LAI from various spectroscopic datasets. Similarly, Ashourloo et al. (2016) concluded that GPR yielded most accurate leaf rust disease detection as compared to VIs, PLSR and SVR. However, GPR is no exception in suffering from radiometric collinearity when many bands are included, and related spectroscopic studies demonstrated that results can be further improved by combining GPR with band selection (Verrelst et al. 2016b) or with dimensionality reduction methods (Rivera-Caicedo et al. 2017). At the same time, alternative GPR versions continue to be developed within the machine learning community. For instance, Lazaro-Gredilla et al. (2014) refined the GPR method by proposing a non-standard variable approximation allowing for accurate inferences in signal-dependent noise scenarios. The so-called variational heteroscedastic GPR (VHGPR) appears to be an excellent alternative for standard GPR, which was demonstrated on a CHRIS dataset where VHGPR outperformed GPR in leaf chlorophyll content estimation. Schematic illustrations of popular nonlinear nonparametric methods are shown in Fig. 5.

4 Physically Based Model Inversion Methods

Physically based model inversion is based on physical laws establishing cause-effect relationships. Inferences on model variables are based on generally accepted knowledge embedded in radiative transfer models (RTMs). RTMs are deterministic models that describe absorption and multiple scattering, and some of them even describe the microwave region, thermal emission or sun-induced chlorophyll fluorescence emitted by vegetation (e.g., see Table 5). A diversity of canopy RTMs have been developed over the last three decades with varying degrees of complexity. Gradual increase in RTMs accuracy, yet in complexity too, has diversified RTMs from simple turbid medium RTMs to advanced Monte Carlo RTMs that allow for explicit 3D representations of complex canopy architectures (e.g., see the RAMI exercises (Pinty et al. 2001, 2004; Widlowski et al. 2007, 2011, 2015) for a thorough comparison). This evolution has resulted in an increase in the computational requirements to run the model, which bears implications towards practical applications. From a computational point of view, RTMs can be categorized as either (1) *economically invertible* (or computationally cheap) or (2) *non-economically invertible* models (or computationally expensive). These terms refer to the model complexity and associated run-time constraining the mathematical inversion of such models. Economically invertible models are models with relatively few input parameters and fast processing that enables fast calculations and consequently fast model inversion or rendering of simulated scenes. A well-known example of this category includes the widely used leaf RTM PROSPECT (Feret et al. 2008) coupled with the canopy RTM SAIL (Verhoef 1984a) [combined named as PROSAIL (Jacquemoud et al. 2009a)].

Non-economically invertible RTMs refer to advanced, computationally expensive RTMs, often with a large number of input variables and sophisticated computational and mathematical modelling. These types of RTMs enable the generation of complex or detailed scenes, but at the expense of a significant computational load. In short, the following families of RTMs can be considered as non-economically invertible: (1) Monte Carlo ray-tracing models [e.g., Raytran (Govaerts and Verstraete 1998)], FLIGHT (North 1996) and librat (Lewis 1999)); (2) voxel-based models [e.g., DART (Gastellu-Etchegorry et al. 1996)]; and (3) advanced integrated vegetation and atmospheric transfer models [e.g., SCOPE (Tol et al. 2009) and MODTRAN (Berk et al. 2006)]. Descriptions of advanced canopy RTM models and their latest developments are provided in Table 5. Although these advanced RTMs serve perfectly as virtual laboratories for fundamental research on light–vegetation interactions, they are in general less suitable for retrieval applications, because of either a large number of input variables or a long processing time. Nevertheless, as outlined below, some experimental studies demonstrated that they can as well be applied into inversion schemes, e.g., based on look-up tables and in hybrid strategies.

Regardless of their complexity, they all deliver spectroscopic outputs, typically at 1 nm resolution. Hence, RTM outputs can fit perfectly into inversion schemes of imaging spectroscopy data, while at the same time the simulated data can be resampled to reassemble the band settings of multispectral sensors. Because inversion strategies are usually based on spectral fitting (i.e. only radiometric information is used), the drawback of collinearity complicating regression is not an issue here; however, removal of noisy bands is still a standard and much-needed preprocessing step to enable adequate spectral fitting. Another point to be mentioned is that inversion scheme can only retrieve the RTM input variables. Hence, using this strategy implies that only RTM state variables can be mapped. Yet because the RTM input variables drive the canopy absorbance and scattering mechanisms, the resulting output maps are considered to be physically sound (Knyazikhin et al. 2013; Myneni et al. 1995) (Fig. 6).

Given that in principle only a coupled leaf-canopy RTM and an inversion routine are required for the retrieval of RTM state variables, the approach is generic and generally applicable. Nevertheless, these approaches are not straightforward. First, an RTM has to be selected, whereby a trade-off between the realism and inversion possibility of the RTM has to be made. As discussed above, typically, complex models are more realistic, but they have many variables and consequently challenging to invert, whereas simpler models may be less realistic but easier to invert. Secondly, according to the Hadamard postulates, RTMs are invertible only when an inversion solution is unique and dependent—in a continuous mode—on the variables to be extracted. Unfortunately, this boundary condition is often not met. The inversion of canopy RTMs is frequently underdetermined and ill-posed. The number of unknowns can be much larger than the number of independent observations. This makes physically based retrievals of vegetation properties a challenging task. Several strategies have been proposed to cope with the underdetermined problem of optimizing the inversion process, including (1) *iterative numerical optimization* methods, (2) *look-up table (LUT)-based inversion* (see Fig. 7 for illustrations), or (3) *hybrid* approaches in which LUTs are generated as input for machine learning approaches (see Sect. 5). Below we briefly

review some common RTM inversion techniques in view of converting spectroscopic data into maps of RTM leaf and canopy input variables.

Numerical optimization. Iterative optimization is a classical technique to invert RTMs in image processing (Botha et al. 2007; Jacquemoud et al. 1995; Zarco-Tejada et al. 2001). The optimization is minimizing a cost function, which estimates the difference between measured and estimated variables by successive input variable iteration. Optimization algorithms are computationally demanding and hence potentially time-consuming depending on the complexity of the RTM and the numbers of image pixels to be processed. However, with the ongoing increase in computational power and open-source availability of optimization libraries, a renaissance of numerical approaches is emerging. Examples of numerical inversion against spectroscopic data include: PROSPECT inversion to retrieve leaf chlorophyll content (Zhang and Wang 2015), retrieval of leaf biochemistry against an improved version of PROSPECT (COSINE) (Jay et al. 2016), and PROSAIL leaf and canopy variables (Bayat et al. 2016; Tol et al. 2016). Despite a gain in computational power, numerical inversion algorithms applied to images are still time-consuming given the many per-pixel iterations and a high number of pixels involved. Hence, in its current form this method stays restricted to computationally fast RTMs in merely experimental settings.

Look-up table (LUT) strategies are based on the generation of simulated spectral reflectance scenarios for a high number of plausible combinations of variable value ranges. As such, the inversion problem is reduced to the identification of the modelled reflectance set that resembles most closely the measured one. This process is based on querying the LUT and applying a cost function. A cost function minimizes the summed differences between simulated and measured reflectances for all wavelengths. The main advantage of LUT-based inversion routines over numerical optimization is their computational speed, since the computationally most demanding part of the inversion procedure is completed before the inversion itself (Dorigo et al. 2007). Consequently, LUT-based inversion methods are typically used as a preferred solution in RTM inversion studies. The classical LUT-based inversion approach is based on a RMSE cost function, which continues to be applied until today. This approach proved to be especially successful for chlorophyll (Kempeneers et al. 2008; Omari et al. 2013; Zhang et al. 2008) and LAI mapping. For instance, by using LUT-based inversion routines imaging spectroscopy data have been processed for the mapping of forest LAI (Banskota et al. 2013, 2015), grassland LAI (Atzberger et al. 2015) and LAI over agricultural crops based on UAVs (Duan et al. 2014). To further mitigate the ill-posed problem and optimize the robustness of the LUT-based inversion routines, a diversity of regularization strategies have been explored in inversion applications against spectroscopic data:

- *The use of prior knowledge* to constrain model variables in the development of a LUT (Baret and Buis 2008; Darvishzadeh et al. 2008; Koetz et al. 2005). Prior knowledge typically involves information on the feasible variable ranges for involved vegetation types (Dorigo et al. 2009; Verrelst et al. 2012c). Prior information together with prior distributions is also increasingly applied into a Bayesian context, whereby the inverted values are generated based on likelihoods (Laurent et al. 2013, 2014; Shiklomanov et al. 2016). The advantage

of a Bayesian framework is its capability to quantify an inversion uncertainty around an inversion variable.

- *Selection of cost function*. The inverse problem of a nonlinear RTM is based on the minimization of a cost function concurrently measuring the discrepancy between (i) observed and simulated reflectance, and (ii) variables to estimate and the associated prior information (Jacquemoud et al. 2009b). To avoid solutions reaching fixed boundaries, a modified cost function in the LUT search that takes uncertainty of provided prior information into account is sometimes used, e.g., by means of the above-mentioned Bayesian approach. Alternatively, Leonenko et al. (2013) proposed and evaluated over 60 different cost functions dealing with different error distributions. Some more spectroscopic studies have evaluated among others the role of cost function (Danner et al. 2017; Locherer et al. 2015) in LUT-based inversion. Although the classical RMSE is a robust cost function, sometimes improvements can be gained with alternative cost functions, e.g., when the LUTs are non-normal distributed.
- The use of *multiple best solutions* in the inversion (mean or median), as opposed to a single best solution (Banskota et al. 2015; Kattenborn et al. 2017; Koetz et al. 2005; Locherer et al. 2015).
- The addition of *artificial noise* (additive or inverse multiplicative white noise) to account for uncertainties linked to measurements and models (Danner et al. 2017; Koetz et al. 2005; Locherer et al. 2015).
- Several spectroscopic studies reported that the relationship between measured and estimated variable perceptibly improves when only specific (sensitive) spectral ranges are selected for model inversion (Darvishzadeh et al. 2012; Meroni et al. 2004; Schlerf et al. 2005). To account for noise in the observations, other spectroscopic studies instead manipulated the observed spectra by applying a smoothing filter (Arellano et al. 2017) or wavelet transforms (Ali et al. 2016; Banskota et al. 2013; Kattenborn et al. 2017). Spectral selection and spectral polishing methods can be applied at the same time in order to enhance the resemblance with the usually more spectrally smooth simulated spectra.

Because of taking sun–target–sensor geometry into account, the use of RTM-based methods has been demonstrated to improve robustness to solar and view angle effects, compared to index-based methods (Kempeneers et al. 2008). Another advantage of RTM inversion routines is that uncertainties are provided as spectral residuals (Rivera et al. 2013) or standard deviations, when mapping multiple solution means (Verrelst et al. 2014). Yet the main drawback lies in its computational burden resulting from too many per-pixel iterations. Although LUT-inversion approaches may speed up the inversion process as opposed to numerical inversion, these inversion routines are still computationally expensive due to the iterative calls of LUT entries on a per-pixel basis. Consequently, despite attempts to optimize inversion algorithms in order to save up computational time for solving inverse radiative transfer problems (Favennec et al. 2016; Gastellu-Etchegorry et al. 2003), in terms of processing speed the RTM inversion routines still run behind statistical methods.

5 Hybrid Regression Methods

Having discussed the more fundamental categories of retrieval methods, this section addresses *hybrid* regression methods. Hybrid methods combine the generalization level of physically based methods with the flexibility and computational efficiency of advanced machine learning methods. This approach replaces the ground data needed for training of the parametric or nonparametric models by RTM input variables, which makes it computationally efficient. It is important to note that the hybrid approach does not alleviate the main issues of RTMs, notably that they only include existing knowledge and concepts. Similarly as in the case of LUT-based inversion, RTM simulations build a LUT representing a broad set of canopy realizations and the hybrid approach uses all available data stored in LUT to train a machine learning regression model (Fig. 8).

The awareness in the mid-1990s that ANNs are excellent algorithms to deal with large datasets led to the introduction of hybrid methods based on ANNs trained with generically applicable RTM-generated data. It led to operational retrieval algorithms for datastreams acquired by multispectral and superspectral sensors [see Verrelst et al. (2015)]. Although this approach is less straightforward in the context of imaging spectroscopy, because of the challenge of collinearity, some recent efforts have been undertaken in exploring this research direction. Noteworthy is the work of Vohland et al. (2010) comparing a numerically optimized ANN with a LUT-based inversion using PROSAIL RTM simulations. Prediction accuracies generally decreased in the following sequence: numerical optimization > LUT > ANN. This would indicate that an ANN may not always be the best choice for inversion applications. However, no dimensionality reduction method was applied, which suggests that the regression model suffered from band collinearity effects. Also Fei et al. (2012) compared a PROSAIL-ANN hybrid approach with a PCA approach. The authors concluded that a PCA transformation into a regression function can mitigate the known reflectance saturation effect of dense canopies to some extent. This PROSAIL-ANN strategy was revisited by Rivera-Caicedo et al. (2017) with alternative dimensionality reduction methods. Although PCA improved accuracies as opposed of using all bands, substantially more improvements were achieved when converting the spectra into components by means canonical correlation analysis (CCA) or orthonormalized PLS (OPLS).

Likewise, inputs from more advanced RTMs were explored to develop specialized hybrid structures. In Malenovský et al. (2013), an ANN was trained based on PROSPECT-DART simulations that explicitly took 3D canopy structures into account to estimate forest leaf chlorophyll content from hyperspectral airborne AISA data. In this approach, the DART simulations went first through a continuum removal transformation. Alternatively, some studies have attempted to move away from ANN models by exploring hybrid structures on the basis of kernel-based machine learning regression algorithms, particularly the popular SVR. For instance, leaf chlorophyll content was estimated based on a PROSAIL-SVR model and applied to imaging spectroscopy (Preidl and Doktor 2011). An analogous concept was applied for a SVR that was trained by PROSPECT-DART simulations in combination with continuum removal transformations, with the purpose of quantifying forest biochemical and structural properties (Homolová and Janoutová 2016). Similarly, Doktor et al. (2014) used a PROSAIL dataset to train a random forest (RF) model to predict LAI and leaf chlorophyll

content, and Liang et al. (2016) compared PROSAIL-based hybrid models with SVR and RF for leaf and canopy chlorophyll content estimation from CHRIS data. Finally, Rivera-Caicedo et al. (2017) analysed ensembles of regression algorithms with dimensionality reduction methods to consolidate the most ideal PROSAIL-based (2101 bands) hybrid regression model. This study concluded that compressing PROSAIL data into CCA or OPLS components led to highest accuracies when trained with a GPR model. Altogether, although these studies have only been developed in experimental settings—similar as the operational multispectral hybrid algorithms (e.g., Bacour et al. 2006; Baret et al. 2013)—the hybrid structures can be perfectly implemented into global mapping schemes. When combined with a dimensionality reduction method to suppress collinearity, hybrid methods have a great potential to advance towards operational spectroscopy-based processing schemes.

6 Discussion

The mapping of spatially continuous biophysical variables from imaging spectroscopy data is a progressively expanding field of research and development thanks to advances in spectrometer technology and in specialized methods interpreting the acquired spectral data. As a follow-up of an earlier, more general review on retrieval methods applicable to optical remote sensing (Verrelst et al. 2015), here a summary on retrieval methods specifically applied to spectroscopic data has been compiled. Four categories have been summarized: (1) parametric, (2) nonparametric, (3) RTM inversion and (4) hybrid methods. The first two categories are statistical methods commonly used with experimental (field) data, whereas the latter two rely on RTM simulations. A schematic flowchart of the main retrieval methods and their hierarchy is provided in Fig. 9.

While pros and cons of each of these methodological categories have been earlier discussed (Verrelst et al. 2015), here we discuss these categories from the perspective of forthcoming routinely acquired and standardized (e.g., atmospherically corrected) imaging spectroscopy data streams. First of all, the choice of a method bears implications, not only on the retrievability and processing time of mappable vegetation properties, but also on the purpose of the retrieval. Parametric and nonparametric methods rely on ground data for training, which obviously need to be available in order to apply these methods. If they are available, they are the ‘shortest’ way to the variables of interest, because especially the nonparametric methods do no impose any limitation on the relationship between the spectrum and the variable of interest. In contrast, RTMs describe radiative transfer processes, i.e. they use existing knowledge (as materialized in the models) rather than ground measured data. Retrieval from an RTM through inversion is most useful if one is more interested in the underlying radiative transfer processes (scattering, sun and shade foliage fractions, light distribution within vegetation canopies, relationships between canopy structure and photosynthesis), rather than in merely extracting a specific variable. However, strategies relying on RTM simulations are inherently limited by the input variables of the RTM and, as discussed in Sect. 4, ancillary data and regularization methods may be required to optimize their inversions.

Statistical approaches, on the other hand, possess the flexibility to relate reflectance data with any measured biophysical variable—state variable or not. As demonstrated

in Sects. 2 and 3, this can be any quantifiable attribute, typically in the domains of leaf biochemical constituents (e.g., nitrogen, phosphorus), pigments (e.g., chlorophyll, carotenoids, xanthophylls) or higher-level structural variables (e.g., above-ground biomass, grain yield). The strength of the correlation with validation data typically determines the validity and transferability of the statistical model. While this 'seeking for best correlations' can be criticized, because of the absence of a physical basis (Knyazikhin et al. 2013), statistical approaches are becoming increasingly powerful to extract biochemical variables through complex and often indirect relationships. Particularly, machine learning models are powerful in extracting information from subtle variations in spectroscopic data through adaptive, nonlinear relationships. The advantage of these statistical models is that not only variable-specific absorption features can be used for information extraction, but also secondary relationships with variables related to other absorption features that co-vary with the variable of interest can be exploited (Ollinger 2011; Verrelst et al. 2012b). Since high accuracies are often obtained with these methods, they are gaining popularity, not only for quantification of a diversity of vegetation properties, but also in mapping of floristic composition (Feilhauer et al. 2017; Harris et al. 2015; Neumann et al. 2016; Roth et al. 2015).

Regardless of the nature of retrieval method, in view of mapping larger areas, and especially in an operational and global context, what matters is the possibility to provide associated information on the retrieval quality. The characterization of uncertainty is a fundamental requirement for postulating correct scientific conclusions from results and for assimilating results into statistical or mechanistic higher-level models (Cressie et al. 2009). As addressed in Sect. 2, parametric regression methods, i.e. spectral transformation methods in combination with a fitting function, do not provide uncertainty estimates, which undermine their applicability to other images in space and time. Subsequently, while valid when locally calibrated and validated, parametric methods are of little use in an operational context. With regard to inversion routines, uncertainties can be provided as spectral residuals (Rivera et al. 2013) or standard deviations when mapping multiple solution means (Verrelst et al. 2014). Lately, inversion approaches were proposed in a Bayesian framework (Shiklomanov et al. 2016), whereby uncertainties are delivered along with the retrievals. In the case of traditional statistical models, uncertainty estimation has been a complex exercise. Statistical models developed within a Bayesian framework, such as GPR, provide uncertainties together with the predictions (Verrelst et al. 2013b; Camps-Valls et al. 2016), which indicate the probability interval of an estimation relative to the samples used during the training phase. These uncertainties can be used to evaluate GPR model transferability. For example, by mapping the uncertainties Verrelst et al. (2013b) demonstrated that a locally developed regression model can be successfully transported to other images in space and time for the large majority of pixels (i.e. the uncertainty maps were not systematically worse). Similarly, uncertainties can inform about the model performance. It was demonstrated that dimensionality reduction methods applied in GPR models for LAI mapping not only largely speed up the processing, but they also led to lower perpixel uncertainties as opposed to mapping using all bands (Rivera-Caicedo et al. 2017). In conclusion, in the view of an operational processing need, just as important as the variable retrieval itself is the provision of an associated uncertainty estimate. Uncertainty estimates

allow evaluating the method's per-pixel performance and consequently allow evaluating the method's capability to process routinely acquired imaging data. They thus provide a measure of the retrieval fidelity, which can be used to identify and mask out the highly uncertain and non-reliable results.

Another important aspect for operational production of vegetation properties from typically bulky imaging spectroscopy data streams implies computational speed. Generally, the lower the complexity of a model, the faster it will be able to produce maps. This highly favors the application of parametric regression approaches since they consist of only few transformations and equations. Also nonparametric regression algorithms, once trained, can be applied to process an image almost instantaneously. Training of machine learning models is frequently related to the tuning of several free variables with costly cross-validation approaches. These scale poorly with the number of samples (such as in kernel machines) or with the data dimensions (such as in ANNs). Although a trained ANN converts an image into a map quasi-instantly, kernel-based methods require more processing time, because the similarity between each test pixel in the image and those used to train the model has to be estimated. Training can be computationally costly, especially when using a big training dataset, e.g., as in hybrid strategies. A solution to shorten training time could be in size reduction of the training data in a way that maximal relevant information is preserved. This can be achieved by means of dimensionality reduction methods in the spectral domain (Rivera-Caicedo et al. 2017), or by means of intelligent sampling in the sampling domain, e.g., through active learning (Verrelst et al. 2016a).

Considerably longer run-time is expected in the case of inversion routines. Since RTMs take some time to generate simulations, especially for computationally expensive models, and also the evaluation takes place on a per-pixel basis, the iterative inversion routines are computationally expensive leading to relatively slow mapping speeds. In an attempt to accelerate their mapping speed, it has been proposed to approximate the functioning of the original RTM by means of statistical learning called *emulation* (Gómez-Dans et al. 2016; Rivera et al. 2015). Initial experiments to emulate leaf, canopy and atmospheric RTMs demonstrated that emulators can successfully generate spectral output from a limited set of input variable almost instantly, thereby preserving sufficient accuracy as compared to the original RTM (Verrelst et al. 2016c, 2017). Although an emulator reproduces RTM simulations instantly, application of a per-pixel spectral fitting requires many repetitions, which implies that these methods still do not reach the speed of statistical methods.

All in all, having the purpose of advancing towards operational imaging spectroscopy data processing in mind, i.e. reaching globally applicable, accurate and fast estimates, we end up with the following recommendations:

- To enable model transferability to routinely acquired images, retrieval methods must provide associated per-pixel uncertainties as a quality indicator whether the model can perform adequately in another space and time.
- Regarding the computational speed, e.g., in case of repetitive image processing, statistical (i.e. regression) methods are multiple times faster than physically

based methods, capable of processing full images in the order of minutes or even seconds.

- In the case of regression methods (experimental or hybrid), multicollinearity of spectroscopic data complicates the development of powerful models. Physically based methods using spectral fitting do not suffer from this problem.
- To mitigate the problem of multicollinearity in regression methods, either band selection or dimensionality reduction methods can be applied before entering the regression. Although band selection is a common practice, more powerful regression models can probably be obtained when using a dimensionality reduction method.

7 Conclusions

With forthcoming imaging spectrometer satellite missions, an unprecedented stream of datasets on the terrestrial biosphere will become available. This will require powerful processing techniques enabling quantification of vegetation variables in an operational and global setting. Four categories of retrieval methods have been discussed in this review paper: (1) parametric regression; (2) nonparametric regression; (3) physically based RTM inversion; and, (4) hybrid methods. For each of these categories, various methodological approaches are increasingly applied to imaging spectroscopy data. This literature review synthesized the current state of the art in the field of spectroscopy-based vegetation properties mapping.

Although parametric methods, such as shape indices or spectral transformation, deal well with extracting relevant information embedded in spectroscopic data, their lack of uncertainty estimates makes them unsuitable for operational use. Higher accuracies can be reached with nonlinear nonparametric methods, especially those in the field of machine learning that generate probabilistic outputs, e.g., Gaussian process regression. However, an additional step to mitigate their spectral multicollinearity is deemed necessary. A popular strategy in this respect is selecting a set of vegetation indices or applying spectral transformation before training the machine learning algorithm. It nevertheless remains questionable whether such band selection approaches fully capture all relevant information. Instead, dimensionality reduction methods that enable compressing the large majority of spectral variability into a few components tend to lead to more accurate predictions.

On the other hand, the inversion of physically based RTMs against spectroscopic data is generally applicable and physically sound, but optimizing their inversion strategies is more challenging compared to the regression methods. RTM-based inversion is computationally demanding, and ancillary information is usually required as an input or to regulate the inversion algorithm. Hybrid regression methods, based on the coupling of an RTM with a machine learning regression algorithm, overcome the problem of processing speed. Particularly, Bayesian kernel-based hybrid strategies possess promising features, as they combine speed, flexibility and the provision of uncertainty estimates. Their accuracies and processing speed can be further improved in combination with dimensionality reduction. Altogether, and in the interest of operational spectroscopy-based mapping of vegetation

Europe PMC Funders Author Manuscripts

properties, we recommend to further explore the feasibility and implementation of hybrid strategies into the next-generation data processing chains.

Acknowledgements

Jochem Verrelst was supported by the European Research Council (ERC) under the ERC-2017-STG SENTIFLEX project (grant agreement 755617). Contribution of Zbyněk Malenovský was supported by the Australian Research Council Future Fellowship: Bridging scales in remote sensing of vegetation stress (FT160100477). Gustau Camps-Valls was supported by the ERC under the ERC-CoG-2014 SEDAL project (grant agreement 647423). We thank the two reviewers for their valuable suggestions.

References

Adam E, Mutanga O, Abdel-Rahman E, Ismail R. Estimating standing biomass in papyrus (Cyperus papyrus L.) swamp: exploratory of in situ hyperspectral indices and random forest regression. Int J Remote Sens. 2014; 35 (2) 693–714.

Addink E, De Jong S, Pebesma E. The importance of scale in object-based mapping of vegetation parameters with hyperspectral imagery. Photogramm Eng Remote Sens. 2007; 73 (8) 905–912.

Ali A, Skidmore A, Darvishzadeh R, van Duren I, Holzwarth S, Mueller J. Retrieval of forest leaf functional traits from HySpex imagery using radiative transfer models and continuous wavelet analysis. ISPRS J Photogramm Remote Sens. 2016; 122: 68–80.

Alton P, Ellis R, Los S, North P. Improved global simulations of gross primary product based on a separate and explicit treatment of diffuse and direct sunlight. J Geophys Res Atmos. 2007; 112 D02108

Arellano P, Tansey K, Balzter H, Tellkamp M. Plant family-specific impacts of petroleum pollution on biodiversity and leaf chlorophyll content in the Amazon rainforest of Ecuador. PLoS ONE. 2017; 12 (1) e0169867 [PubMed: 28103307]

Arenas-García J, Camps-Valls G. Efficient kernel orthonormalized PLS for remote sensing applications. IEEE Trans Geosci Remote Sens. 2008; 46 (10) 2872–2881.

Ashourloo D, Aghighi H, Matkan A, Mobasheri M, Rad A. An investigation into machine learning regression techniques for the leaf rust disease detection using hyperspectral measurement. IEEE J Select Top Appl Earth Observ Remote Sens. 2016; 9 (9) 4344–4351.

Atzberger C, Guérif M, Baret F, Werner W. Comparative analysis of three chemometric techniques for the spectroradiometric assessment of canopy chlorophyll content in winter wheat. Comput Electron Agric. 2010; 73 (2) 165–173.

Atzberger C, Darvishzadeh R, Immitzer M, Schlerf M, Skidmore A, le Maire G. Comparative analysis of different retrieval methods for mapping grassland leaf area index using airborne imaging spectroscopy. Int J Appl Earth Observ Geoinf. 2015; 43: 19–31.

Bacour C, Baret F, Béal D, Weiss M, Pavageau K. Neural network estimation of LAI, fAPAR, fCover and LAI×Cab, from top of canopy MERIS reflectance data: principles and validation. Remote Sens Environ. 2006; 105 (4) 313–325.

Balzarolo M, Vescovo L, Hammerle A, Gianelle D, Papale D, Tomelleri E, Wohlfahrt G. On the relationship between ecosystem-scale hyperspectral reflectance and CO_2 exchange in European mountain grasslands. Biogeosciences. 2015; 12 (10) 3089–3108.

Banskota A, Wynne R, Thomas V, Serbin S, Kayastha N, Gastellu-Etchegorry J, Townsend P. Investigating the utility of wavelet transforms for inverting a 3-D radiative transfer model using hyperspec-tral data to retrieve forest LAI. Remote Sens. 2013; 5 (6) 2639–2659.

Banskota A, Serbin S, Wynne R, Thomas V, Falkowski M, Kayastha N, Gastellu-Etchegorry JP, Townsend P. An LUT-based inversion of DART model to estimate forest LAI from hyperspectral data. IEEE J Sel Top Appl Earth Observ Remote Sens. 2015; 8 (6) 3147–3160.

Bao S, Cao C, Chen W, Tian H. Spectral features and separability of alpine wetland grass species. Spectrosc Lett. 2017; 50 (5) 245–256.

Baranoski G, Rokne J. A practical approach for estimating the red edge position of plant leaf reflectance. Int J Remote Sens. 2005; 26 (3) 503–521.

Europe PMC Funders Author Manuscripts

Baret, F, Buis, S. Advances in land remote sensing: system, modeling, inversion and application. Liang, S, editor. Springer; New York: 2008. 171–200.

Baret F, Weiss M, Lacaze R, Camacho F, Makhmara H, Pacholcyzk P, Smets B. GEOV1: LAI and FAPAR essential climate variables and FCOVER global time series capitalizing over existing products. Part 1: principles of development and production. Remote Sens Environ. 2013; 137: 299–309.

Barton CVM, North P. Remote sensing of canopy light use efficiency using the photochemical reflectance index: model and sensitivity analysis. Remote Sens Environ. 2001; 78 (3) 264–273.

Bayat B, van der Tol C, Verhoef W. Remote sensing of grass response to drought stress using spectroscopic techniques and canopy reflectance model inversion. Remote Sens. 2016; 8 (7) 557

Belgiu M, Drăguţ L. Random forest in remote sensing: a review of applications and future directions. ISPRS J Photogramm Remote Sens. 2016; 114: 24–31.

Berk A, Anderson G, Acharya P, Bernstein L, Muratov L, Lee J, Fox M, Adler-Golden S, Chetwynd J, Hoke M, Lockwood R, et al. MODTRAN™ 5: 2006 update. 2006; 6233

Botha E, Leblon B, Zebarth B, Watmough J. Non-destructive estimation of potato leaf chlorophyll from canopy hyperspectral reflectance using the inverted PROSAIL model. Int J Appl Earth Observ Geoinf. 2007; 9 (4) 360–374.

Bratsch S, Epstein H, Buchhorn M, Walker D, Landes H. Relationships between hyperspectral data and components of vegetation biomass in Low Arctic tundra communities at Ivotuk, Alaska. Environ Res Lett. 2017; 12 (2) 025003

Breiman L. Bagging predictors. Mach Learn. 1996; 24 (2) 123–140.

Breiman L. Random forests. Mach Learn. 2001; 45 (1) 5–32.

Breiman, L, Friedman, J, Stone, C, Olshen, R. Classification and regression trees The Wadsworth and Brooks-Cole statistics-probability series. Taylor & Francis; London: 1984.

Broge NH, Leblanc E. Comparing prediction power and stability of broadband and hyperspectral vegetation indices for estimation of green leaf area index and canopy chlorophyll density. Remote Sens Environ. 2001; 76 (2) 156–172.

Broomhead, DS, Lowe, D. Radial basis functions, multi-variable functional interpolation and adaptive networks Tech rep. Royal Signals and Radar Establishment Malvern (United Kingdom); 1988.

Buchhorn M, Walker DA, Heim B, Raynolds MK, Epstein HE, Schwieder M. Ground-based hyperspectral characterization of alaska tundra vegetation along environmental gradients. Remote Sens. 2013; 5 (8) 3971–4005.

Burden F, Winkler D. Robust QSAR models using bayesian regularized neural networks. J Med Chem. 1999; 42 (16) 3183–3187. [PubMed: 10447964]

Bye I, North P, Los S, Kljun N, Rosette J, Hopkinson C, Chasmer L, Mahoney C. Estimating forest canopy parameters from satellite waveform LiDAR by inversion of the FLIGHT three-dimensional radiative transfer model. Remote Sens Environ. 2017; 188: 177–189.

Camps-Valls G, Verrelst J, Muñoz-Marí J, Laparra V, Mateo-Jiménez F, Gómez-Dans J. A survey on Gaussian processes for earth observation data analysis. IEEE Geosci Remote Sens Mag. 2016; 4 (2) 41–57.

Capolupo A, Kooistra L, Berendonk C, Boccia L, Suomalainen J. Estimating plant traits of grasslands from UAV-acquired hyperspectral images: a comparison of statistical approaches. ISPRS Int J Geo-Inf. 2015; 4 (4) 2792–2820.

Chen B, Wu Z, Wang J, Dong J, Guan L, Chen J, Yang K, Xie G. Spatio-temporal prediction of leaf area index of rubber plantation using HJ-1A/1B CCD images and recurrent neural network. ISPRS J Photogramm Remote Sens. 2015; 102: 148–160.

Cho MA, Skidmore AK. A new technique for extracting the red edge position from hyperspectral data: the linear extrapolation method. Remote Sens Environ. 2006; 101 (2) 181–193.

Cho M, Skidmore A, Corsi F, van Wieren S, Sobhan Ib. Estimation of green grass/herb biomass from airborne hyperspectral imagery using spectral indices and partial least squares regression. Int J Appl Earth Observ Geoinf. 2007; 9 (4) 414–424.

Cho MA, Skidmore AK, Atzberger C. Towards red-edge positions less sensitive to canopy biophysical parameters for leaf chlorophyll estimation using properties optique spectrales des feuilles

(PROSPECT) and scattering by arbitrarily inclined leaves (SAILH) simulated data. Int J Remote Sens. 2008; 29 (8) 2241–2255.

Clark RN, Roush TL. Reflectance spectroscopy: quantitative analysis techniques for remote sensing applications. J Geophys Res Solid Earth. 1984; 89 (B7) 6329–6340.

Clevers J. Beyond NDVI: extraction of biophysical variables from remote sensing imagery. Remote Sens Digital Image Process. 2014; 18: 363–381.

Clevers J, Kooistra L. Using hyperspectral remote sensing data for retrieving canopy chlorophyll and nitrogen content. IEEE J Sel Top Appl Earth Observ Remote Sens. 2012; 5 (2) 574–583.

Clevers JGPW, Kooistra L, Salas EAL. Study of heavy metal contamination in river floodplains using the red-edge position in spectroscopic data. Int J Remote Sens. 2004; 25 (19) 3883–3895.

Coops NC, Smith ML, Martin M, Ollinger SV. Prediction of eucalypt foliage nitrogen content from satellite-derived hyperspectral data. IEEE Trans Geosci Remote Sens. 2003; 41 (6) 1338–1346.

Cressie N, Calder C, Clark J, Ver Hoef J, Wikle C. Accounting for uncertainty in ecological analysis: the strengths and limitations of hierarchical statistical modeling. Ecol Appl. 2009; 19 (3) 553–570. [PubMed: 19425416]

Danner M, Berger K, Wocher M, Mauser W, Hank T. Retrieval of biophysical crop variables from multi-angular canopy spectroscopy. Remote Sens. 2017; 9 (7) 726

Darvishzadeh R, Skidmore A, Schlerf M, Atzberger C. Inversion of a radiative transfer model for estimating vegetation LAI and chlorophyll in a heterogeneous grassland. Remote Sens Environ. 2008; 112 (5) 2592–2604.

Darvishzadeh R, Matkan AA, Dashti Ahangar A. Inversion of a radiative transfer model for estimation of rice canopy chlorophyll content using a lookup-table approach. IEEE J Sel Top Appl Earth Observ Remote Sens. 2012; 99: 1–9.

Dawson T, Curran P, Plummer S. LIBERTY—Modeling the effects of leaf biochemical concentration on reflectance spectra. Remote Sens Environ. 1998; 65 (1) 50–60.

Delegido J, Alonso L, González G, Moreno J. Estimating chlorophyll content of crops from hyperspectral data using a normalized area over reflectance curve (NAOC). Int J Appl Earth Observ Geoinf. 2010; 12 (3) 165–174.

Delegido J, Verrelst J, Alonso L, Moreno J. Evaluation of sentinel-2 red-edge bands for empirical estimation of green LAI and chlorophyll content. Sensors. 2011; 11 (7) 7063–7081. [PubMed: 22164004]

Delegido J, Verrelst J, Meza C, Rivera J, Alonso L, Moreno J. A red-edge spectral index for remote sensing estimation of green LAI over agroecosystems. Eur J Agron. 2013; 46: 42–52.

Dietz A, Kuenzer C, Gessner U, Dech S. Remote sensing of snow—a review of available methods. Int J Remote Sens. 2012; 33 (13) 4094–4134.

Disney M, Lewis P, Saich P. 3D modelling of forest canopy structure for remote sensing simulations in the optical and microwave domains. Remote Sens Environ. 2006; 100 (1) 114–132.

Doktor D, Lausch A, Spengler D, Thurner M. Extraction of plant physiological status from hyperspectral signatures using machine learning methods. Remote Sens. 2014; 6 (12) 12247–12274.

Dorigo WA, Zurita-Milla R, de Wit AJW, Brazile J, Singh R, Schaepman ME. A review on reflective remote sensing and data assimilation techniques for enhanced agroecosystem modeling. Int J Appl Earth Observ Geoinf. 2007; 9 (2) 165–193.

Dorigo W, Richter R, Baret F, Bamler R, Wagner W. Enhanced automated canopy characterization from hyperspectral data by a novel two step radiative transfer model inversion approach. Remote Sens. 2009; 1 (4) 1139–1170.

Draper, NR, Smith, H. Applied regression analysis. Wiley; New York: 2014.

Dreccer M, Barnes L, Meder R. Quantitative dynamics of stem water soluble carbohydrates in wheat can be monitored in the field using hyperspectral reflectance. Field Crops Res. 2014; 159: 70–80.

Drusch M, Moreno J, Del Bello U, Franco R, Goulas Y, Huth A, Kraft S, Middleton EM, Miglietta F, Mohammed G, et al. The fluorescence explorer mission concept-ESA's earth explorer 8. IEEE Trans Geosci Remote Sens. 2017; 55 (3) 1273–1284.

Du L, Shi S, Yang J, Sun J, Gong W. Using different regression methods to estimate leaf nitrogen content in rice by fusing hyperspectral LiDAR data and laser-induced chlorophyll fluorescence data. Remote Sens. 2016; 8 (6) 526

Duan SB, Li ZL, Wu H, Tang BH, Ma L, Zhao E, Li C. Inversion of the PROSAIL model to estimate leaf area index of maize, potato, and sunflower fields from unmanned aerial vehicle hyperspectral data. Int J Appl Earth Observ Geoinf. 2014; 26 (1) 12–20.

Elvidge CD, Chen Z. Comparison of broad-band and narrow-band red and near-infrared vegetation indices. Remote Sens Environ. 1995; 54 (1) 38–48.

Favennec Y, Le Hardy D, Dubot F, Rousseau B, Rousse D. Some speed-up strategies for solving inverse radiative transfer problems. J Phys Conf Ser. 2016; 676 (1) 012006

Fei Y, Jiulin S, Hongliang F, Zuofang Y, Jiahua Z, Yunqiang Z, Kaishan S, Zongming W, Maogui H. Comparison of different methods for corn LAI estimation over northeastern China. Int J Appl Earth Observ Geoinf. 2012; 18: 462–471.

Feilhauer H, Asner GP, Martin RE. Multi-method ensemble selection of spectral bands related to leaf biochemistry. Remote Sens Environ. 2015; 164: 57–65.

Feilhauer H, Somers B, van der Linden S. Optical trait indicators for remote sensing of plant species composition: predictive power and seasonal variability. Ecol Indic. 2017; 73: 825–833.

Feng H, Yang F, Li Z, Yang G, Guo J, He P, Wang Y. Hyperspectral estimation of leaf total phosphorus content in apple tree based on optimal weights combination model. Nongye Gongcheng Xuebao/ Trans Chin Soc Agric Eng. 2016; 32 (7) 173–180.

Feret JB, François C, Asner GP, Gitelson AA, Martin RE, Bidel LPR, Ustin SL, le Maire G, Jacquemoud S. PROSPECT-4 and 5: advances in the leaf optical properties model separating photosynthetic pigments. Remote Sens Environ. 2008; 112 (6) 3030–3043.

Foster A, Kakani V, Mosali J. Estimation of bioenergy crop yield and N status by hyperspectral canopy reflectance and partial least square regression. Precis Agric. 2017; 18 (2) 192–209.

Francl L, Panigrahi S. Artificial neural network models of wheat leaf wetness. Agric For Meteorol. 1997; 88 (1-4) 57–65.

Friedman J, Hastie T, Tibshirani R. Additive logistic regression: a statistical view of boosting. Ann Stat. 2000; 28 (2) 337–407.

Fu Y, Yang G, Feng H, Xu X, Song X, Wang J. Comparison of winter wheat LAI estimation methods based on hyperspectral dimensionality reduction and vegetation index. Nongye Gongcheng Xuebao/ Trans Chin Soc Agric Eng. 2012; 28 (23) 107–113.

Gastellu-Etchegorry J, Demarez V, Pinel V, Zagolski F. Modeling radiative transfer in heterogeneous 3-D vegetation canopies. Remote Sens Environ. 1996; 58 (2) 131–156.

Gastellu-Etchegorry J, Guillevic P, Zagolski F, Demarez V, Trichon V, Deering D, Leroy M. Modeling BRF and radiation regime of boreal and tropical forests: I BRF. Remote Sens Environ. 1999; 68 (3) 281–316.

Gastellu-Etchegorry J, Gascon F, Esteve P. An interpolation procedure for generalizing a look-up table inversion method. Remote Sens Environ. 2003; 87 (1) 55–71.

Gastellu-Etchegorry J, Martin E, Gascon F. DART: a 3D model for simulating satellite images and studying surface radiation budget. Int J Remote Sens. 2004; 25 (1) 73–96.

Gastellu-Etchegorry JP, Yin T, Lauret N, Cajgfinger T, Gregoire T, Grau E, Feret JB, Lopes M, Guilleux J, Dedieu G, Malenovský Z, et al. Discrete anisotropic radiative transfer (DART 5) for modeling airborne and satellite spectro-radiometer and LIDAR acquisitions of natural and urban landscapes. Remote Sens. 2015; 7 (2) 1667–1701.

Gastellu-Etchegorry JP, Yin T, Lauret N, Grau E, Rubio J, Cook B, Morton D, Sun G. Simulation of satellite, airborne and terrestrial LiDAR with DART (I): Waveform simulation with quasi-Monte Carlo ray tracing. Remote Sens Environ. 2016; 184: 418–435.

Gastellu-Etchegorry J, Lauret N, Yin T, Landier L, Kallel A, Malenovský Z, Al Bitar A, Aval J, Benhmida S, Qi J, Medjdoub G, et al. DART: recent advances in remote sensing data modeling with atmosphere, polarization, and chlorophyll fluorescence. IEEE J Sel Top Appl Earth Observ Remote Sens. 2017.

Geladi P, Kowalski B. Partial least-squares regression: a tutorial. Analytica Chimica Acta. 1986; 185 (C) 1–17.

Gewali U, Monteiro S, Saber E. Machine learning based hyperspectral image analysis: a survey. 2018. arXiv:180208701

Gianelle D, Guastella F. Nadir and off-nadir hyperspectral field data: strengths and limitations in estimating grassland biophysical characteristics. Int J Remote Sens. 2007; 28 (7) 1547–1560.

Glenn E, Huete A, Nagler P, Nelson S. Relationship between remotely-sensed vegetation indices, canopy attributes and plant physiological processes: What vegetation indices can and cannot tell us about the landscape. Sensors. 2008; 8 (4) 2136–2160. [PubMed: 27879814]

Gómez-Chova, L, Muñoz-Marí, J, Laparra, V, Malo-López, J, Camps-Valls, G. Optical remote sensing. Springer; Berlin: 2011. 171–206.

Gómez-Dans JL, Lewis PE, Disney M. Efficient emulation of radiative transfer codes using gaussian processes and application to land surface parameter inferences. Remote Sens. 2016; 8 (2) 119

Gonsamo A. Normalized sensitivity measures for leaf area index estimation using three-band spectral vegetation indices. Int J Remote Sens. 2011; 32 (7) 2069–2080.

Govaerts YM, Verstraete MM. Raytran: a Monte Carlo ray-tracing model to compute light scattering in three-dimensional heterogeneous media. IEEE Trans Geosci Remote Sens. 1998; 36 (2) 493–505.

Grau E, Gastellu-Etchegorry JP. Radiative transfer modeling in the Earth-Atmosphere system with DART model. Remote Sens Environ. 2013; 139: 149–170.

Guanter L, Kaufmann H, Segl K, Foerster S, Rogass C, Chabrillat S, Kuester T, Hollstein A, Rossner G, Chlebek C, Straif C, et al. The EnMAP spaceborne imaging spectroscopy mission for earth observation. Remote Sens. 2015; 7 (7) 8830

Guillevic P, Gastellu-Etchegorry J, Demarty J, Prévot L. Thermal infrared radiative transfer within three-dimensional vegetation covers. J Geophys Res Atmos. 2003; doi: 10.1029/2002JD002247

Han ZY, Zhu XC, Fang XY, Wang ZY, Wang L, Zhao GX, Jiang YM. Hyperspectral estimation of apple tree canopy LAI based on SVM and RF regression. Guang Pu Xue Yu Guang Pu Fen Xi/Spec-trosc Spectr Anal. 2016; 36 (3) 800–805.

Hancock S, Lewis P, Foster M, Disney M, Muller JP. Measuring forests with dual wavelength lidar: a simulation study over topography. Agric For Meteorol. 2012; 161: 123–133.

Hansen PM, Schjoerring JK. Reflectance measurement of canopy biomass and nitrogen status in wheat crops using normalized difference vegetation indices and partial least squares regression. Remote Sens Environ. 2003; 86 (4) 542–553.

Harris A, Charnock R, Lucas R. Hyperspectral remote sensing of peatland floristic gradients. Remote Sens Environ. 2015; 162: 99–111.

Haykin, S. Neural networks—a comprehensive foundation. 2nd edn. Prentice Hall; Upper Saddle: 1999.

He R, Qiao X, Jiang J, Guo H. Retrieving canopy leaf total nitrogen content of winter wheat by continuous wavelet transform. Nongye Gongcheng Xuebao/Trans Chin Soc Agric Eng. 2015; 31 (2) 141–146.

Heiskanen J, Rautiainen M, Stenberg P, Mõttus M, Vesanto VH. Sensitivity of narrowband vegetation indices to boreal forest LAI, reflectance seasonality and species composition. ISPRS J Photogramm Remote Sens. 2013; 78: 1–14.

Hernández-Clemente R, North P, Hornero A, Zarco-Tejada P. Assessing the effects of forest health on sun-induced chlorophyll fluorescence using the FluorFLIGHT 3-D radiative transfer model to account for forest structure. Remote Sens Environ. 2017; 193: 165–179.

Hochreiter S, Schmidhuber J. Long short-term memory. Neural Comput. 1997; 9 (8) 1735–1780. [PubMed: 9377276]

Homolová L, Janoutová R, Malenovský Z. Evaluation of various spectral inputs for estimation of forest biochemical and structural properties from airborne imaging spectroscopy data. 2016; 41: 961–966.

Huang Z, Turner BJ, Dury SJ, Wallis IR, Foley WJ. Estimating foliage nitrogen concentration from HYMAP data using continuum removal analysis. Remote Sens Environ. 2004; 93 (1) 18–29.

Huang Y, Tian Q, Wang L, Geng J, Lyu C. Estimating canopy leaf area index in the late stages of wheat growth using continuous wavelet transform. J Appl Remote Sens. 2014; 8 (1) 083517

Hughes G. On the mean accuracy of statistical pattern recognizers. IEEE Trans Inf Theory. 1968; 14 (1) 55–63.

Im J, Jensen JR, Coleman M, Nelson E. Hyperspectral remote sensing analysis of short rotation woody crops grown with controlled nutrient and irrigation treatments. Geocarto Int. 2009; 24 (4) 293–312.

Jacquemoud S, Baret F, Andrieu B, Danson FM, Jaggard K. Extraction of vegetation biophysical parameters by inversion of the PROSPECT+SAIL models on sugar beet canopy reflectance data. Application to TM and AVIRIS sensors. Remote Sens Environ. 1995; 52 (3) 163–172.

Jacquemoud S, Verhoef W, Baret F, Bacour C, Zarco-Tejada P, Asner G, François C, Ustin S. PROSPECT + SAIL models: a review of use for vegetation characterization. Remote Sens Environ. 2009a; 113 (SUPPL 1) S56–S66.

Jacquemoud S, Verhoef W, Baret F, Bacour C, Zarco-Tejada P, Asner G, François C, Ustin S. PROSPECT + SAIL models: a review of use for vegetation characterization. Remote Sens Environ. 2009b; 113 (SUPPL 1) S56–S66.

Jay S, Bendoula R, Hadoux X, Féret JB, Gorretta N. A physically-based model for retrieving foliar biochemistry and leaf orientation using close-range imaging spectroscopy. Remote Sens Environ. 2016; 177: 220–236.

Jensen R, Hardin P, Hardin A. Estimating urban leaf area index (LAI) of individual trees with hyper-spectral data. Photogramm Eng Remote Sens. 2012; 78 (5) 495–504.

Jia F, Liu G, Liu D, Zhang Y, Fan W, Xing X. Comparison of different methods for estimating nitrogen concentration in flue-cured tobacco leaves based on hyperspectral reflectance. Field Crops Res. 2013; 150: 108–114.

Kalacska M, Lalonde M, Moore T. Estimation of foliar chlorophyll and nitrogen content in an ombrotrophic bog from hyperspectral data: Scaling from leaf to image. Remote Sens Environ. 2015; 169: 270–279.

Kanke Y, Tubaña B, Dalen M, Harrell D. Evaluation of red and red-edge reflectance-based vegetation indices for rice biomass and grain yield prediction models in paddy fields. Precis Agric. 2016; 17 (5) 507–530.

Karimi Y, Prasher S, Madani A, Kim S. Application of support vector machine technology for the estimation of crop biophysical parameters using aerial hyperspectral observations. Can Biosyst Eng/ Le Genie des biosystems au Canada. 2008; 50: 7.13–7.20.

Kattenborn T, Fassnacht F, Pierce S, Lopatin J, Grime J, Schmidtlein S. Linking plant strategies and plant traits derived by radiative transfer modelling. J Veg Sci. 2017; 28 (4) 717–727.

Kempeneers P, Zarco-Tejada PJ, North PRJ, de Backer S, Delalieux S, Sepulcre-Cantó G, Morales F, van Aardt JAN, Sagardoy R, Coppin P, Scheunders P. Model inversion for chlorophyll estimation in open canopies from hyperspectral imagery. Int J Remote Sens. 2008; 29 (17–18) 5093–5111.

Kiala Z, Odindi J, Mutanga O, Peerbhay K. Comparison of partial least squares and support vector regressions for predicting leaf area index on a tropical grassland using hyperspectral data. J Appl Remote Sens. 2016; 10 (3) 036015

Kimes DS, Nelson RF, Manry MT, Fung AK. Attributes of neural networks for extracting continuous vegetation variables from optical and radar measurements. Int J Remote Sens. 1998; 19 (14) 2639–2662.

Kira O, Nguy-Robertson A, Arkebauer T, Linker R, Gitelson A. Informative spectral bands for remote green LAI estimation in C3 and C4 crops. Agric For Meteorol. 2016; 218–219: 243–249.

Knox N, Skidmore A, Prins H, Asner G, van der Werff H, de Boer W, van der Waal C, de Knegt H, Kohi E, Slotow R, Grant R. Dry season mapping of savanna forage quality, using the hyperspectral Carnegie Airborne Observatory sensor. Remote Sens Environ. 2011; 115 (6) 1478–1488.

Knyazikhin Y, Schull MA, Stenberg P, Mõttus M, Rautiainen M, Yang Y, Marshak A, Carmona PL, Kaufmann RK, Lewis P, et al. Hyperspectral remote sensing of foliar nitrogen content. Proc Natl Acad Sci. 2013; 110 (3) E185–E192. [PubMed: 23213258]

Koetz B, Baret F, Poilvé H, Hill J. Use of coupled canopy structure dynamic and radiative transfer models to estimate biophysical canopy characteristics. Remote Sens Environ. 2005; 95 (1) 115–124.

Kováč D, Malenovský Z, Urban O, Špunda V, Kalina J, Ač A, Kaplan V, Hanuš J. Response of green reflectance continuum removal index to the xanthophyll de-epoxidation cycle in norway spruce needles. J Exp Bot. 2013; 64 (7) 1817–1827. [PubMed: 23564955]

Labate D, Ceccherini M, Cisbani A, De Cosmo V, Galeazzi C, Giunti L, Melozzi M, Pieraccini S, Stagi M. The PRISMA payload optomechanical design: a high performance instrument for a new hyperspectral mission. Acta Astronautica. 2009; 65 (9–10) 1429–1436.

Laurent V, Verhoef W, Damm A, Schaepman M, Clevers J. A Bayesian object-based approach for estimating vegetation biophysical and biochemical variables from APEX at-sensor radiance data. Remote Sens Environ. 2013; 139: 6–17.

Laurent V, Schaepman M, Verhoef W, Weyermann J, Chávez R. Bayesian object-based estimation of LAI and chlorophyll from a simulated Sentinel-2 top-of-atmosphere radiance image. Remote Sens Environ. 2014; 140: 318–329.

Lazaridis DC, Verbesselt J, Robinson AP. Penalized regression techniques for prediction: a case study for predicting tree mortality using remotely sensed vegetation indices. Can J For Res. 2010; 41 (1) 24–34.

Lazaro-Gredilla M, Titsias M, Verrelst J, Camps-Valls G. Retrieval of biophysical parameters with heteroscedastic Gaussian processes. IEEE Geosci Remote Sens Lett. 2014; 11 (4) 838–842.

le Maire G, François C, Dufrene E. Towards universal broad leaf chlorophyll indices using PROSPECT simulated database and hyperspectral reflectance measurements. Remote Sens Environ. 2004; 89 (1) 1–28.

le Maire G, François C, Soudani K, Berveiller D, Pontailler JY, Bréda N, Genet H, Davi H, Dufrêne E. Calibration and validation of hyperspectral indices for the estimation of broadleaved forest leaf chlorophyll content, leaf mass per area, leaf area index and leaf canopy biomass. Remote Sens Environ. 2008; 112 (10) 3846–3864.

Lee CM, Cable ML, Hook SJ, Green RO, Ustin SL, Mandl DJ, Middleton EM. An introduction to the NASA hyperspectral infrared imager (HyspIRI) mission and preparatory activities. Remote Sens Environ. 2015; 167: 6–19. DOI: 10.1016/j.rse.2015.06.012

Leonenko G, North P, Los S. Statistical distances and their applications to biophysical parameter estimation: information measures, M-estimates, and minimum contrast methods. Remote Sens. 2013; 5 (3) 1355–1388.

Lewis P. Three-dimensional plant modelling for remote sensing simulation studies using the botanical plant modelling system. Agronomie. 1999; 19 (3–4) 185–210.

Lewis P, Muller J. The advanced radiometric ray tracer: ararat for plant canopy reflectance simulation. Int Arch Photogramm Remote Sens. 1993; 29: 26–26.

Lewis, P; Muller, J. Botanical plant modelling for remote sensing simulation studies; 10th Annual International on Geoscience and Remote Sensing Symposium, 1990. IGARSS'90.'Remote Sensing Science for the Nineties'; 1990. 1739–1742.

Li L, Zhang Q, Huang D. A review of imaging techniques for plant phenotyping. Sensors (Switzerland). 2014a; 14 (11) 20078–20111.

Li X, Liu X, Liu M, Wu L. Random forest algorithm and regional applications of spectral inversion model for estimating canopy nitrogen concentration in rice. Yaogan Xuebao/J Remote Sens. 2014b; 18 (4) 934–945.

Li D, Cheng T, Zhou K, Zheng H, Yao X, Tian Y, Zhu Y, Cao W. WREP: a wavelet-based technique for extracting the red edge position from reflectance spectra for estimating leaf and canopy chlorophyll contents of cereal crops. ISPRS J Photogramm Remote Sens. 2017; 129: 103–117.

Liang L, Di L, Zhang L, Deng M, Qin Z, Zhao S, Lin H. Estimation of crop LAI using hyperspec-tral vegetation indices and a hybrid inversion method. Remote Sens Environ. 2015; 165: 123–134.

Liang L, Qin Z, Zhao S, Di L, Zhang C, Deng M, Lin H, Zhang L, Wang L, Liu Z. Estimating crop chlorophyll content with hyperspectral vegetation indices and the hybrid inversion method. Int J Remote Sens. 2016; 37 (13) 2923–2949.

Lin H, Liang L, Zhang L, Du P. Wheat leaf area index inversion with hyperspectral remote sensing based on support vector regression algorithm. Nongye Gongcheng Xuebao/Trans Chin Soc Agric Eng. 2013; 29 (11) 139–146.

Liu WY, Pan J. A hyperspectral assessment model for leaf chlorophyll content of Pinus masso-niana based on neural network. Chin J Appl Ecol. 2017; 28 (4) 1128–1136.

Locherer M, Hank T, Danner M, Mauser W. Retrieval of seasonal leaf area index from simulated EnMAP data through optimized LUT-based inversion of the PROSAIL model. Remote Sens. 2015; 7 (8) 10321–10346.

Luo J, Huang W, Zhao J, Zhang J, Zhao C, Ma R. Detecting aphid density of winter wheat leaf using hyperspectral measurements. IEEE J Sel Top Appl Earth Observ Remote Sens. 2013; 6 (2) 690–698.

Malenovský Z, Ufer C, Lhotakova Z, Clevers J, Schaepman M, Albrechtova J, Cudlin P. A new hyperspectral index for chlorophyll estimation of a forest canopy: area under curve normalised to maximal band depth between 650 and 725 nm. EARSeL EProc. 2006; 5 (2) 161–172.

Malenovský Z, Homolová L, Zurita-Milla R, Lukeš P, Kaplan V, Hanuš J, Gastellu-Etchegorry JP, Schaepman ME. Retrieval of spruce leaf chlorophyll content from airborne image data using continuum removal and radiative transfer. Remote Sens Environ. 2013; 131: 85–102.

Malenovský Z, Turnbull JD, Lucieer A, Robinson SA. Antarctic moss stress assessment based on chlorophyll content and leaf density retrieved from imaging spectroscopy data. New Phytol. 2015; 208 (2) 608–624. [PubMed: 26083501]

Malenovský Z, Lucieer A, King DH, Turnbull JD, Robinson SA. Unmanned aircraft system advances health mapping of fragile polar vegetation. Methods Ecol Evol. 2017; 8 (12) 1842–1857.

Marabel M, Alvarez-Taboada F. Spectroscopic determination of aboveground biomass in grasslands using spectral transformations, support vector machine and partial least squares regression. Sensors (Switzerland). 2013; 13 (8) 10027–10051.

Mariotto I, Thenkabail P, Huete A, Slonecker E, Platonov A. Hyperspectral versus multispectral crop-productivity modeling and type discrimination for the HyspIRI mission. Remote Sens Environ. 2013; 139: 291–305.

Marshall M, Thenkabail P. Biomass modeling of four leading world crops using hyperspectral narrowbands in support of HyspIRI mission. Photogramm Eng Remote Sens. 2014; 80 (8) 757–772.

Matthes J, Knox S, Sturtevant C, Sonnentag O, Verfaillie J, Baldocchi D. Predicting landscapescale CO2 flux at a pasture and rice paddy with long-term hyperspectral canopy reflectance measurements. Biogeosciences. 2015; 12 (15) 4577–4594.

Matthews M. A current review of empirical procedures of remote sensing in inland and nearcoastal transitional waters. Int J Remote Sens. 2011; 32 (21) 6855–6899.

Meroni M, Colombo R, Panigada C. Inversion of a radiative transfer model with hyperspectral observations for LAI mapping in poplar plantations. Remote Sens Environ. 2004; 92 (2) 195–206.

Miller J, Hare E, Wu J. Quantitative characterization of the vegetation red edge reflectance 1. An inverted-Gaussian reflectance model. Remote Sens. 1990; 11 (10) 1755–1773.

Miphokasap P, Honda K, Vaiphasa C, Souris M, Nagai M. Estimating canopy nitrogen concentration in sugarcane using field imaging spectroscopy. Remote Sens. 2012; 4 (6) 1651–1670.

Mitchell JJ, Glenn NF, Sankey TT, Derryberry DR, Germino MJ. Remote sensing of sagebrush canopy nitrogen. Remote Sens Environ. 2012; 124: 217–223.

Montesano P, Rosette J, Sun G, North P, Nelson R, Dubayah R, Ranson K, Kharuk V. The uncertainty of biomass estimates from modeled ICESat-2 returns across a boreal forest gradient. Remote Sens Environ. 2015; 158: 95–109.

Morton DC, Nagol J, Carabajal CC, Rosette J, Palace M, Cook BD, Vermote EF, Harding DJ, North PR. Amazon forests maintain consistent canopy structure and greenness during the dry season. Nature. 2014; 506 (7487) 221–224. [PubMed: 24499816]

Mulder V, de Bruin S, Schaepman M, Mayr T. The use of remote sensing in soil and terrain mapping—a review. Geoderma. 2011; 162 (1-2) 1–19.

Mutanga O, Kumar L. Estimating and mapping grass phosphorus concentration in an African savanna using hyperspectral image data. Int J Remote Sens. 2007; 28 (21) 4897–4911.

Mutanga O, Skidmore AK. Narrow band vegetation indices overcome the saturation problem in biomass estimation. Int J Remote Sens. 2004; 25 (19) 3999–4014.

Mutanga O, Skidmore AK, Kumar L, Ferwerda J. Estimating tropical pasture quality at canopy level using band depth analysis with continuum removal in the visible domain. Int J Remote Sens. 2005; 26 (6) 1093–1108.

Myneni R, Maggion S, Iaquinta J, Privette J, Gobron N, Pinty B, Kimes D, Verstraete M, Williams D. Optical remote sensing of vegetation: modeling, caveats, and algorithms. Remote Sens Environ. 1995; 51 (1) 169–188.

Neinavaz E, Skidmore A, Darvishzadeh R, Groen T. Retrieval of leaf area index in different plant species using thermal hyperspectral data. ISPRS J Photogramm Remote Sens. 2016; 119: 390–401.

Neumann C, Förster M, Kleinschmit B, Itzerott S. Utilizing a PLSR-based band-selection procedure for spectral feature characterization of floristic gradients. IEEE J Sel Top Appl Earth Observ Remote Sens. 2016; 9 (9) 3982–3996.

North P. Three-dimensional forest light interaction model using a monte carlo method. IEEE Trans Geosci Remote Sens. 1996; 34 (4) 946–956.

North P, Rosette J, Suárez J, Los S. A Monte Carlo radiative transfer model of satellite waveform LiDAR. Int J Remote Sens. 2010; 31 (5) 1343–1358.

Ollinger S. Sources of variability in canopy reflectance and the convergent properties of plants. New Phytol. 2011; 189 (2) 375–394. [PubMed: 21083563]

Omari K, White H, Staenz K, King D. Retrieval of forest canopy parameters by inversion of the proflair leaf-canopy reflectance model using the lut approach. IEEE J Sel Top Appl Earth Observ Remote Sens. 2013; 6 (2) 715–723.

Oppelt N, Mauser W. Hyperspectral monitoring of physiological parameters of wheat during a vegetation period using avis data. Int J Remote Sens. 2004; 25 (1) 145–159.

Paruelo J, Tomasel F. Prediction of functional characteristics of ecosystems: a comparison of artificial neural networks and regression models. Ecol Model. 1997; 98 (2-3) 173–186.

Pasqualotto N, Delegido J, Wittenberghe SV, Verrelst J, Rivera JP, Moreno J. Retrieval of canopy water content of different crop types with two new hyperspectral indices: water absorption area index and depth water index. Int J Appl Earth Observ Geoinf. 2018; 67: 69–78.

Peng Y, Huang H, Wang W, Wu J, Wang X. Rapid detection of chlorophyll content in corn leaves by using least squares-support vector machines and hyperspectral images. Jiangsu Daxue Xuebao (Ziran Kexue Ban)/J Jiangsu Univ (Nat Sci Edn). 2011; 32 (2) 125–128.

Penuelas J, Gamon JA, Fredeen AL, Merino J, Field CB. Reflectance indices associated with physiological changes in nitrogen-and water-limited sunflower leaves. Remote Sens Environ. 1994; 48 (2) 135–146.

Pham T, Yoshino K, Bui D. Biomass estimation of Sonneratia caseolaris (l.) Engler at a coastal area of Hai Phong city (Vietnam) using ALOS-2 PALSAR imagery and GIS-based multi-layer perceptron neural networks. GISci Remote Sens. 2017; 54 (3) 329–353.

Pinty B, Gobron N, Widlowski JL, Gerstl S, Verstraete M, Antunes M, Bacour C, Gascon F, Gastellu JP, Goel N, Jacquemoud S, et al. Radiation transfer model intercomparison (RAMI) exercise. J Geophys Res D Atmos. 2001; 106 (D11) 11937–11956.

Pinty B, Widlowski JL, Taberner M, Gobron N, Verstraete M, Disney M, Gascon F, Gastellu JP, Jiang L, Kuusk A, Lewis P, et al. Radiation Transfer Model Intercomparison (RAMI) exercise: results from the second phase. J Geophys Res D Atmos. 2004; 109 (6) D06210

Pôças I, Gonçalves J, Costa P, Gonçalves I, Pereira L, Cunha M. Hyperspectral-based predictive modelling of grapevine water status in the Portuguese Douro wine region. Int J Appl Earth Observ Geoinf. 2017; 58: 177–190.

Preidl, S; Doktor, D. Comparison of radiative transfer model inversions to estimate vegetation physiological status based on hyperspectral data; 3rd workshop on hyperspectral image and signal processing: evolution in remote sensing (WHISPERS); 2011.

Pu R, Gong P, Biging GS, Larrieu MR. Extraction of red edge optical parameters from Hyperion data for estimation of forest leaf area index. IEEE Trans Geosci Remote Sens. 2003; 41 (4) 916–921.

Pullanagari R, Kereszturi G, Yule I. Mapping of macro and micro nutrients of mixed pastures using airborne AisaFENIX hyperspectral imagery. ISPRS J Photogramm Remote Sens. 2016; 117: 1–10.

Ramoelo A, Skidmore AK, Schlerf M, Mathieu R, Heitkönig IM. Water-removed spectra increase the retrieval accuracy when estimating savanna grass nitrogen and phosphorus concentrations. ISPRS J Photogramm Remote Sens. 2011; 66 (4) 408–417.

Rasmussen, CE, Williams, CKI. Gaussian processes for machine learning. The MIT Press; New York: 2006.

Rivard B, Feng J, Gallie A, Sanchez-Azofeifa A. Continuous wavelets for the improved use of spectral libraries and hyperspectral data. Remote Sens Environ. 2008; 112 (6) 2850–2862.

Rivera Caicedo J, Verrelst J, Muñoz-Marí J, Moreno J, Camps-Valls G. Toward a semiautomatic machine learning retrieval of biophysical parameters. IEEE J Sel Top Appl Earth Observ Remote Sens. 2014; 7 (4) 1249–1259.

Rivera J, Verrelst J, Leonenko G, Moreno J. Multiple cost functions and regularization options for improved retrieval of leaf chlorophyll content and LAI through inversion of the PROSAIL model. Remote Sens. 2013; 5 (7) 3280–3304.

Rivera J, Verrelst J, Delegido J, Veroustraete F, Moreno J. On the semi-automatic retrieval of biophysical parameters based on spectral index optimization. Remote Sens. 2014; 6 (6) 4924–4951.

Rivera JP, Verrelst J, Gómez-Dans J, Muñoz Marí J, Moreno J, Camps-Valls G. An emulator toolbox to approximate radiative transfer models with statistical learning. Remote Sens. 2015; 7 (7) 9347

Rivera-Caicedo JP, Verrelst J, Muñoz-Marí J, Camps-Valls G, Moreno J. Hyperspectral dimensionality reduction for biophysical variable statistical retrieval. ISPRS J Photogramm Remote Sens. 2017; 132: 88–101.

Roelofsen HD, Kooistra L, van Bodegom PM, Verrelst J, Krol J, Witte JPM. Mapping a priori defined plant associations using remotely sensed vegetation characteristics. Remote Sens Environ. 2014; 140: 639–651.

Roth K, Roberts D, Dennison P, Alonzo M, Peterson S, Beland M. Differentiating plant species within and across diverse ecosystems with imaging spectroscopy. Remote Sens Environ. 2015; 167: 135–151.

Saich P, Lewis P, Disney M, Thackrah G. Comparison of Hymap/E-SAR data with models for optial reflectance and microwave scattering from vegetation canopies. Retriev Bio Geo Phys Parameters SAR Data Land Appl. 2002; 475: 75–80.

Sanches I, Souza Filho C, Kokaly R. Spectroscopic remote sensing of plant stress at leaf and canopy levels using the chlorophyll 680 nm absorption feature with continuum removal. ISPRS J Photogramm Remote Sens. 2014; 97: 111–122.

Scafutto R, de Souza Filho C, Rivard B. Characterization of mineral substrates impregnated with crude oils using proximal infrared hyperspectral imaging. Remote Sens Environ. 2016; 179: 116–130.

Schlerf M, Atzberger C. Inversion of a forest reflectance model to estimate structural canopy variables from hyperspectral remote sensing data. Remote Sens Environ. 2006; 100 (3) 281–294.

Schlerf M, Atzberger C, Hill J. Remote sensing of forest biophysical variables using HyMap imaging spectrometer data. Remote Sens Environ. 2005; 95 (2) 177–194.

Schlerf M, Atzberger C, Hill J, Buddenbaum H, Werner W, Schüler G. Retrieval of chlorophyll and nitrogen in Norway spruce (Picea abies L. Karst.) using imaging spectroscopy. Int J Appl Earth Observ Geoinf. 2010; 12 (1) 17–26.

Shiklomanov A, Dietze M, Viskari T, Townsend P, Serbin S. Quantifying the influences of spectral resolution on uncertainty in leaf trait estimates through a Bayesian approach to RTM inversion. Remote Sens Environ. 2016; 183: 226–238.

Sims DA, Gamon JA. Relationships between leaf pigment content and spectral reflectance across a wide range of species, leaf structures and developmental stages. Remote Sens Environ. 2002; 81 (2-3) 337–354.

Stimson HC, Breshears DD, Ustin SL, Kefauver SC. Spectral sensing of foliar water conditions in two co-occurring conifer species: Pinus edulis and Juniperus monosperma. Remote Sens Environ. 2005; 96 (1) 108–118.

Suykens J, Vandewalle J. Least squares support vector machine classifiers. Neural Process Lett. 1999; 9 (3) 293–300.

Thenkabail P, Smith R, De Pauw E. Hyperspectral vegetation indices and their relationships with agricultural crop characteristics. Remote Sens Environ. 2000; 71 (2) 158–182.

Tian Y, Yao X, Yang J, Cao W, Zhu Y. Extracting red edge position parameters from ground-and space-based hyperspectral data for estimation of canopy leaf nitrogen concentration in rice. Plant Product Sci. 2011; 14 (3) 270–281.

Tibshirani R. Regression shrinkage and selection via the lasso. J R Stat Soc Ser B (Methodological). 1996; 58: 267–288.

Tuia D, Verrelst J, Alonso L, Pérez-Cruz F, Camps-Valls G. Multioutput support vector regression for remote sensing biophysical parameter estimation. IEEE Geosci Remote Sens Lett. 2011; 8 (4) 804–808.

Tuia, D, Volpi, M, Verrelst, J, Camps-Valls, G. Mathematical models for remote sensing image processing Signals and communication technology. Moser, G, Zerubia, J, editors. Springer; Cham: 2018. 399–441.

Uno Y, Prasher S, Lacroix R, Goel P, Karimi Y, Viau A, Patel R. Artificial neural networks to predict corn yield from compact airborne spectrographic imager data. Comput Electron Agric. 2005; 47 (2) 149–161.

Vaglio Laurin G, Cheung-Wai Chan J, Chen Q, Lindsell J, Coomes D, Guerriero L, Del Frate F, Migli-etta F, Valentini R. Biodiversity mapping in a tropical West African forest with airborne hyperspectral data. PLoS ONE. 2014; 9 (6) e97910 [PubMed: 24937407]

Van Der Tol C, Verhoef W, Timmermans J, Verhoef A, Su Z. An integrated model of soil-canopy spectral radiances, photosynthesis, fluorescence, temperature and energy balance. Biogeosciences. 2009; 6 (12) 3109–3129.

Van Der Tol C, Berry J, Campbell P, Rascher U. Models of fluorescence and photosynthesis for interpreting measurements of solar-induced chlorophyll fluorescence. J Geophys Res Biogeosci. 2014; 119: 2312–2327. [PubMed: 27398266]

van der Tol C, Rossini M, Cogliati S, Verhoef W, Colombo R, Rascher U, Mohammed G. A model and measurement comparison of diurnal cycles of sun-induced chlorophyll fluorescence of crops. Remote Sens Environ. 2016; 186: 663–677.

Vapnik V, Golowich S, Smola A. Support vector method for function approximation, regression estimation, and signal processing. Adv Neural Inf Process Syst. 1997; 9: 281–287.

Verhoef W. Light scattering by leaf layers with application to canopy reflectance modeling: the SAIL model. Remote Sens Environ. 1984a; 16 (2) 125–141.

Verhoef W. Light scattering by leaf layers with application to canopy reflectance modeling: the SAIL model. Remote Sens Environ. 1984b; 16 (2) 125–141.

Verhoef W. Earth observation modeling based on layer scattering matrices. Remote Sens Environ. 1985; 17 (2) 165–178.

Verrelst J, Schaepman M, Koetz B, Kneubuhler M. Angular sensitivity analysis of vegetation indices derived from CHRIS/PROBA data. Remote Sens Environ. 2008; 112 (5) 2341–2353.

Verrelst J, Schaepman ME, Malenovský Z, Clevers JGPW. Effects of woody elements on simulated canopy reflectance: implications for forest chlorophyll content retrieval. Remote Sens Environ. 2010; 114 (3) 647–656.

Verrelst J, Alonso L, Camps-Valls G, Delegido J, Moreno J. Retrieval of vegetation biophysical parameters using Gaussian process techniques. IEEE Trans Geosci Remote Sens. 2012a; 50 (5 PART 2) 1832–1843.

Verrelst J, Alonso L, Camps-Valls G, Delegido J, Moreno J. Retrieval of vegetation biophysical parameters using Gaussian process techniques. IEEE Trans Geosci Remote Sens. 2012b; 50 (5 PART 2) 1832–1843.

Verrelst J, Romijn E, Kooistra L. Mapping vegetation density in a heterogeneous river floodplain ecosystem using pointable CHRIS/PROBA data. Remote Sens. 2012c; 4 (9) 2866–2889.

Verrelst J, Alonso L, Rivera Caicedo J, Moreno J, Camps-Valls G. Gaussian process retrieval of chlorophyll content from imaging spectroscopy data. IEEE J Sel Top Appl Earth Observ Remote Sens. 2013a; 6 (2) 867–874.

Verrelst J, Rivera J, Moreno J, Camps-Valls G. Gaussian processes uncertainty estimates in experimental Sentinel-2 LAI and leaf chlorophyll content retrieval. ISPRS J Photogramm Remote Sens. 2013b; 86: 157–167.

Verrelst J, Rivera J, Leonenko G, Alonso L, Moreno J. Optimizing LUT-based RTM inversion for semiautomatic mapping of crop biophysical parameters from sentinel-2 and-3 data: role of cost functions. IEEE Trans Geosci Remote Sens. 2014; 52 (1) 257–269.

Verrelst J, Camps-Valls G, Muñoz Marí J, Rivera J, Veroustraete F, Clevers J, Moreno J. Optical remote sensing and the retrieval of terrestrial vegetation bio-geophysical properties—a review. ISPRS J Photogramm Remote Sens. 2015; 108: 273–290.

Verrelst J, Dethier S, Rivera JP, Munoz-Mari J, Camps-Valls G, Moreno J. Active learning methods for efficient hybrid biophysical variable retrieval. IEEE Geosci Remote Sens Lett. 2016a; 13 (7) 1012–1016.

Verrelst J, Rivera JP, Gitelson A, Delegido J, Moreno J, Camps-Valls G. Spectral band selection for vegetation properties retrieval using Gaussian processes regression. Int J Appl Earth Observ Geoinf. 2016b; 52: 554–567.

Verrelst J, Sabater N, Rivera JP, Muñoz Marí J, Vicent J, Camps-Valls G, Moreno J. Emulation of leaf, canopy and atmosphere radiative transfer models for fast global sensitivity analysis. Remote Sens. 2016c; 8 (8) 673

Verrelst J, Rivera Caicedo J, Muñoz Marí J, Camps-Valls G, Moreno J. SCOPE-based emulators for fast generation of synthetic canopy reflectance and sun-induced fluorescence Spectra. Remote Sens. 2017; 9 (9) 927

Vilfan N, van der Tol C, Muller O, Rascher U, Verhoef W. Fluspect-B: a model for leaf fluorescence, reflectance and transmittance spectra. Remote Sens Environ. 2016; 186: 596–615.

Vohland M, Mader S, Dorigo W. Applying different inversion techniques to retrieve stand variables of summer barley with PROSPECT + SAIL. Int J Appl Earth Observ Geoinf. 2010; 12 (2) 71–80.

Wang F, Huang J, Lou Z. A comparison of three methods for estimating leaf area index of paddy rice from optimal hyperspectral bands. Precis Agric. 2011; 12 (3) 439–447.

Wang F, Huang J, Wang Y, Liu Z, Peng D, Cao F. Monitoring nitrogen concentration of oilseed rape from hyperspectral data using radial basis function. Int J Digital Earth. 2013; 6 (6) 550–562.

Wang J, Wang T, Skidmore A, Shi T, Wu G. Evaluating different methods for grass nutrient estimation from canopy hyperspectral reflectance. Remote Sens. 2015; 7 (5) 5901–5917.

Wang B, Chen J, Ju W, Qiu F, Zhang Q, Fang M, Chen F. Limited effects of water absorption on reducing the accuracy of leaf nitrogen estimation. Remote Sens. 2017a; 9 (3) 291

Wang J, Shen C, Liu N, Jin X, Fan X, Dong C, Xu Y. Non-destructive evaluation of the leaf nitrogen concentration by in-field visible/near-infrared spectroscopy in pear orchards. Sensors (Switzerland). 2017b; 17 (3) 538

Widlowski JL, Pinty B, Clerici M, Dai Y, De Kauwe M, De Ridder K, Kallel A, Kobayashi H, Lavergne T, Ni-Meister W, Olchev A, et al. RAMI4PILPS: an intercomparison of formulations for the partitioning of solar radiation in land surface models. J Geophys Res G Biogeosci. 2011; doi: 10.1029/2010JG001511

Widlowski JL, Taberner M, Pinty B, Bruniquel-Pinel V, Disney M, Fernandes R, Gastellu-Etchegorry JP, Gobron N, Kuusk A, Lavergne T, Leblanc S, et al. Third radiation transfer model intercomparison (RAMI) exercise: documenting progress in canopy reflectance models. J Geophys Res D Atmos. 2007; 112 (9) D09111

Widlowski JL, Mio C, Disney M, Adams J, Andredakis I, Atzberger C, Brennan J, Busetto L, Chelle M, Ceccherini G, et al. The fourth phase of the radiative transfer model intercomparison (RAMI) exercise: actual canopy scenarios and conformity testing. Remote Sens Environ. 2015; 169: 418–437.

Wold S, Esbensen K, Geladi P. Principal component analysis. Chemom Intell Lab Syst. 1987; 2 (1–3) 37–52.

Xue J, Su B. Significant remote sensing vegetation indices: a review of developments and applications. J Sens. 2017; doi: 10.1155/2017/1353691

Yang X, Huang J, Wu Y, Wang J, Wang P, Wang X, Huete A. Estimating biophysical parameters of rice with remote sensing data using support vector machines. Sci China Life Sci. 2011; 54 (3) 272–281. [PubMed: 21416328]

Yang P, Verhoef W, van der Tol C. The mSCOPE model: a simple adaptation to the SCOPE model to describe reflectance, fluorescence and photosynthesis of vertically heterogeneous canopies. Remote Sens Environ. 2017; 201: 1–11.

Yao X, Huang Y, Shang G, Zhou C, Cheng T, Tian Y, Cao W, Zhu Y. Evaluation of six algorithms to monitor wheat leaf nitrogen concentration. Remote Sens. 2015; 7 (11) 14939–14966.

Ye X, Sakai K, Manago M, Asada SI, Sasao A. Prediction of citrus yield from airborne hyper-spectral imagery. Precis Agric. 2007; 8 (3) 111–125.

Yi Q, Jiapaer G, Chen J, Bao A, Wang F. Different units of measurement of carotenoids estimation in cotton using hyperspectral indices and partial least square regression. ISPRS J Photogramm Remote Sens. 2014; 91: 72–84.

Yin T, Lauret N, Gastellu-Etchegorry JP. Simulation of satellite, airborne and terrestrial LiDAR with DART (II): ALS and TLS multi-pulse acquisitions, photon counting, and solar noise. Remote Sens Environ. 2016; 184: 454–468.

Yue J, Yang G, Li C, Li Z, Wang Y, Feng H, Xu B. Estimation of winter wheat above-ground biomass using unmanned aerial vehicle-based snapshot hyperspectral sensor and crop height improved models. Remote Sens. 2017; 9 (7) 708

Zandler H, Brenning A, Samimi C. Quantifying dwarf shrub biomass in an arid environment: comparing empirical methods in a high dimensional setting. Remote Sens Environ. 2015; 158: 140–155.

Zarco-Tejada P, Miller J, Noland T, Mohammed G, Sampson P. Scaling-up and model inversion methods with narrowband optical indices for chlorophyll content estimation in closed forest canopies with hyperspectral data. IEEE Trans Geosci Remote Sens. 2001; 39 (7) 1491–1507.

Zarco-Tejada P, Miller J, Mohammed G, Noland T, Sampson P. Vegetation stress detection through chlorophyll+ estimation and fluorescence effects on hyperspectral imagery. J Environ Qual. 2002; 31 (5) 1433–1441. [PubMed: 12371159]

Zhang S, Wang Q. Inverse retrieval of chlorophyll from reflected spectra for assimilating branches of drought-tolerant Tamarix ramosissima. IEEE J Sel Top Appl Earth Observ Remote Sens. 2015; 8 (4) 1498–1505.

Zhang Y, Chen J, Miller J, Noland T. Leaf chlorophyll content retrieval from airborne hyperspectral remote sensing imagery. Remote Sens Environ. 2008; 112 (7) 3234–3247.

Europe PMC Funders Author Manuscripts

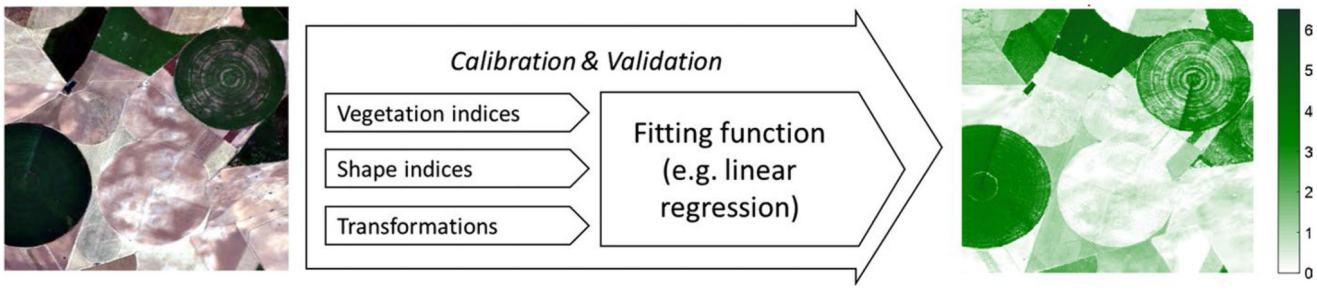

Figure 1.

Principles of parametric regression. Left: red, green, blue (RGB) subset of a hyperspectral HyMap image (125 bands) over Barrax agricultural site (Spain). Right: illustrative map of a vegetation property (leaf area index (LAI), m^2/m^2) as obtained by a two-band normalized difference index and linear regression. The model was validated with a squared correlation coefficient, R^2 of 0.89 (RMSE: 0.63; NRMSE 10.1%). It took 0.2 s to produce the map using ARTMO's SI toolbox (Rivera et al. 2014). No uncertainty estimates are provided

Europe PMC Funders Author Manuscripts

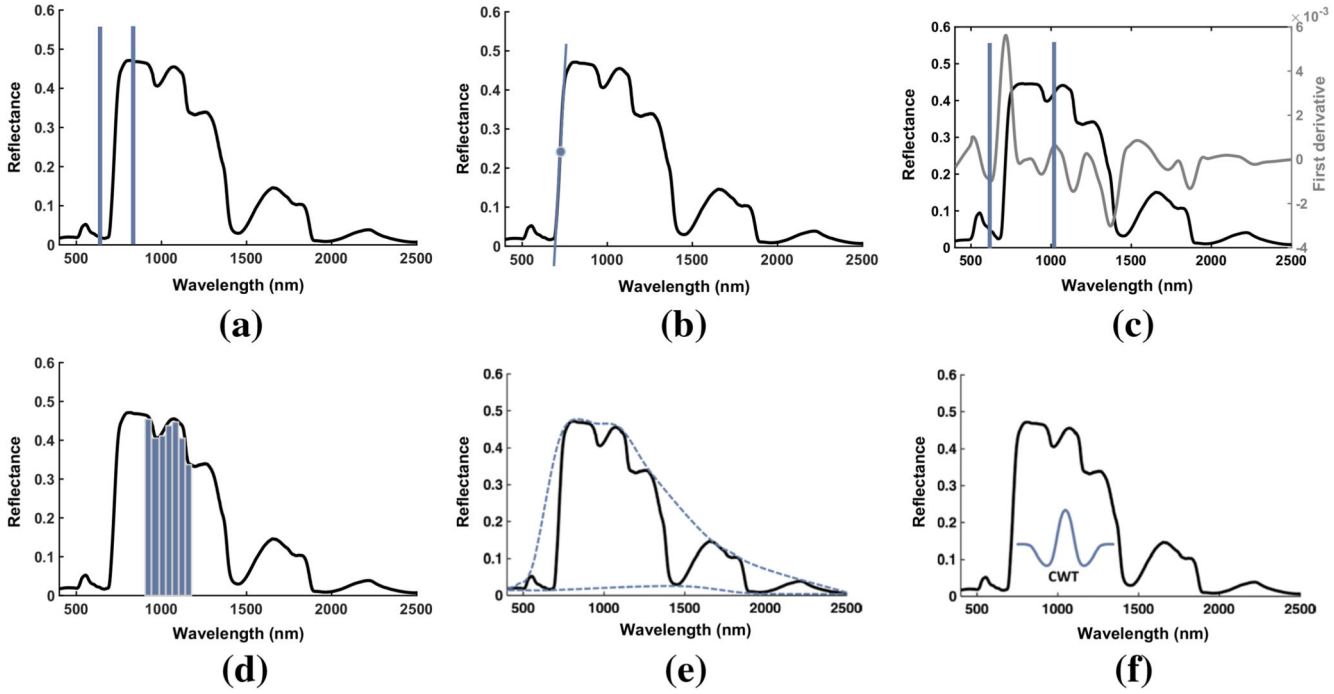

Figure 2.

Schematic illustrations of parametric regression methods: spectral indices (**a**), red-edge position (REP) calculation (**b**), derivative-based indices (**c**), integral-based indices (**d**), continuum removal (**e**) and wavelet transform (**f**). Note that a fitting function is still required to convert transformations towards a biophysical variable

Europe PMC Funders Author Manuscripts

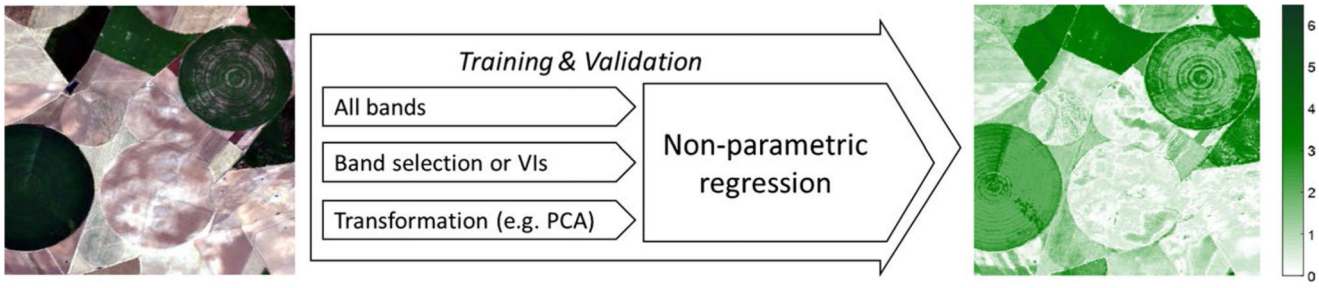

Figure 3.

Principles of nonparametric regression. Left: red, green, blue (RGB) subset of a hyperspectral HyMap image (125 bands) over Barrax agricultural site (Spain). Right: illustrative map of a vegetation property (leaf area index (LAI), m^2/m^2) as obtained by PROSAIL with Gaussian processes regression (GPR). The model was validated with a squared correlation coefficient, R^2 of 0.94 (RMSE: 0.39; NRMSE: 6.3%). It took 5.7 s to produce the map using ARTMO's MLRA toolbox (Rivera Caicedo et al. 2014). With GPR also uncertainty estimates are provided (not shown)

Europe PMC Funders Author Manuscripts

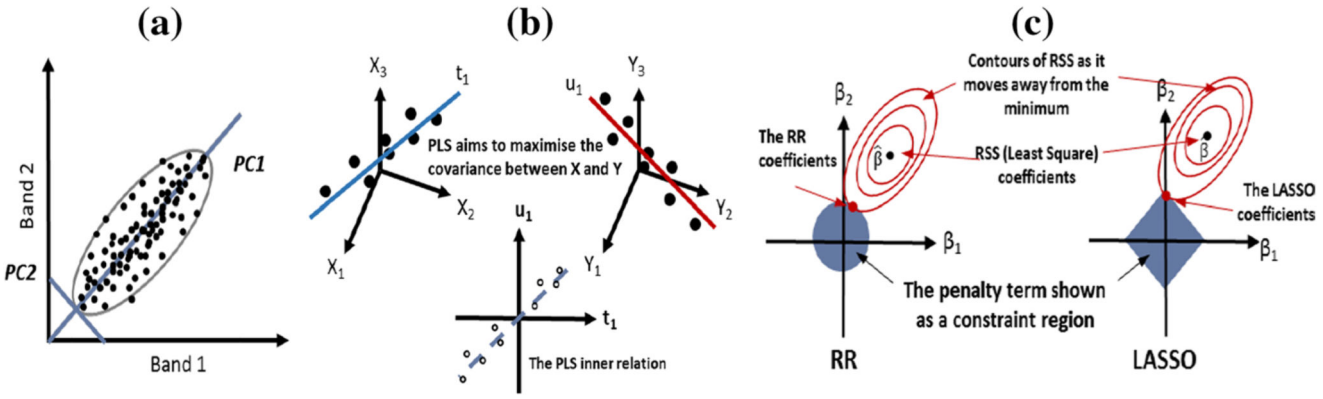

Figure 4.

Schematic illustrations of principal component (PC) (**a**), partial least squares (PLS) (**b**), ridge regression and LASSO (**c**). PC and PLS are combined with a linear regression model

Europe PMC Funders Author Manuscripts

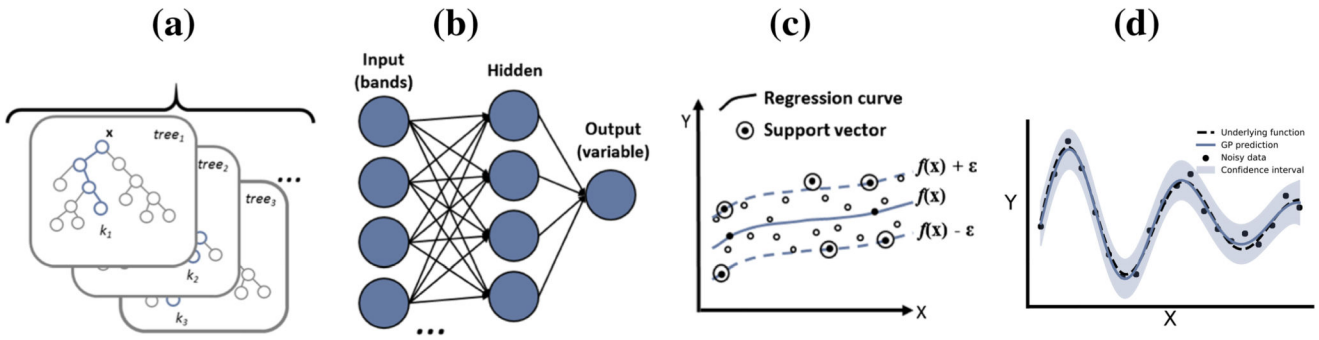

Figure 5.

Schematic illustrations of random forest (RF) (**a**), neural network (NN) (**b**), support vector regression (SVR) (**c**) and Gaussian processes regression (GPR) (**d**)

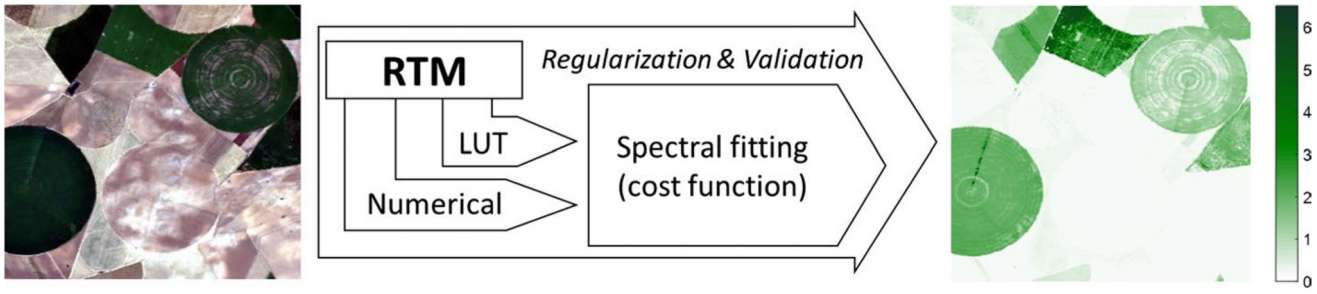

Figure 6.

Principles of radiative transfer model (RTM) inversion. Left: RGB subset of a hyperspectral HyMap image (125 bands) over Barrax agricultural site (Spain). Right: illustrative map of a vegetation property (LAI, m^2/m^2) as obtained by RMSE inversion against a 100,000 PROSAIL LUT (5% noise added, mean of 5% multiple solutions). The model was validated with a R^2 of 0.44 (RMSE: 1.85; NRMSE: 31.9%). A systematic underestimation occurred, which in principle implies that the RTM simulated LUT needs to be better parameterized. It took 2315 s to produce the map using ARTMO's LUT-based inversion toolbox (Rivera et al. 2013). Also uncertainty estimates are provided, e.g., in the form of residuals (not shown)

Europe PMC Funders Author Manuscripts

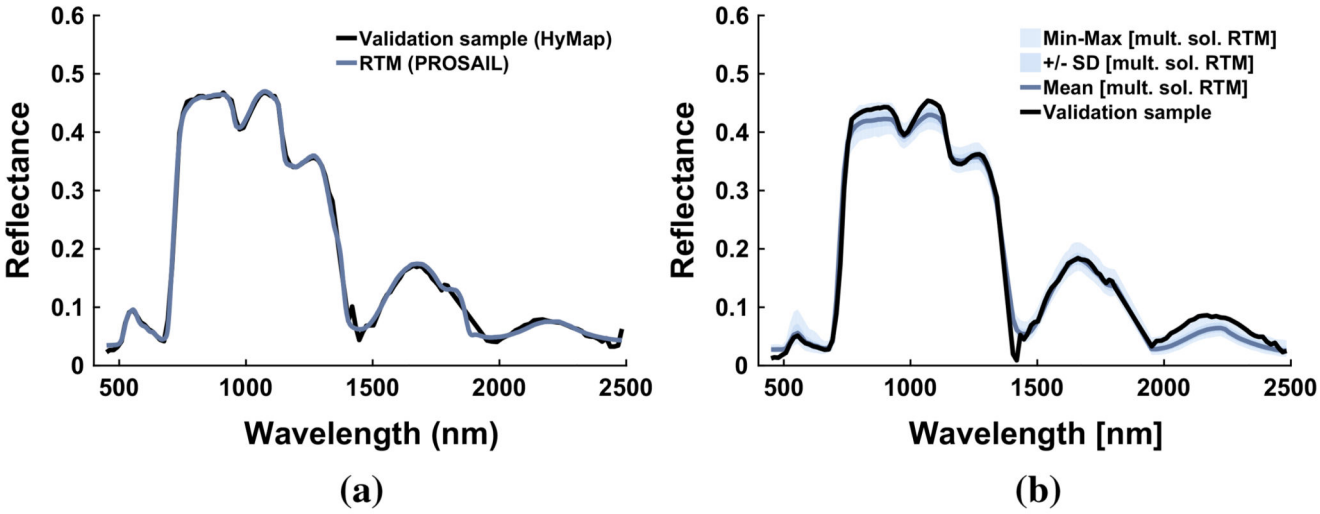

Figure 7.

Illustrations of numerical inversion (**a**) and LUT-based inversion (**b**). A HyMaP spectrum was inverted against PROSAIL. In the case of LUT-inversion, overview statistics of 5% best multiple solutions are shown

Europe PMC Funders Author Manuscripts

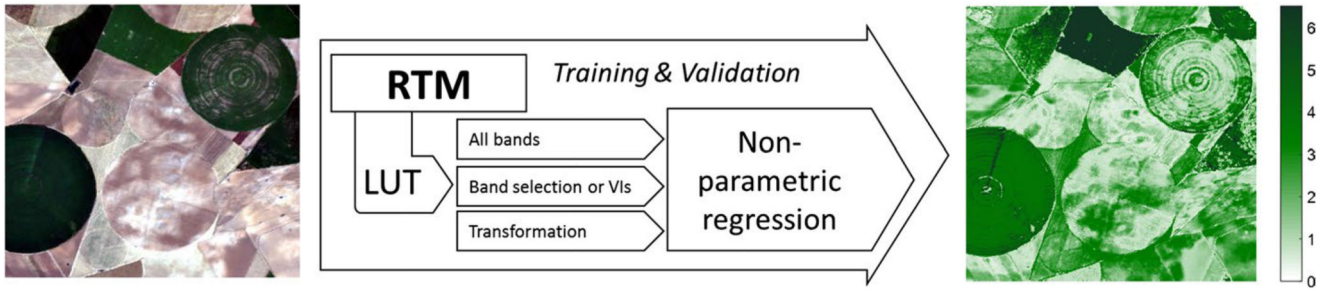

Figure 8.

Principles of hybrid regression. Left: RGB subset of a hyperspectral HyMap image (125 bands) over Barrax agricultural site (Spain). Right: illustrative map of a vegetation property (LAI, m^2/m^2) as obtained by PROSAIL with Gaussian processes regression (GPR) and 15% white noise added. The model was validated with a R^2 of 0.88 (RMSE: 0.70; NRMSE: 10.1%). It took 6.3 seconds to produce the map using ARTMO's MLRA toolbox (Rivera Caicedo et al. 2014). With GPR also uncertainty estimates are provided (not shown). Because of not being trained with bare soil spectra, LAI over the non-irrigated parcels is over-estimated

Europe PMC Funders Author Manuscripts

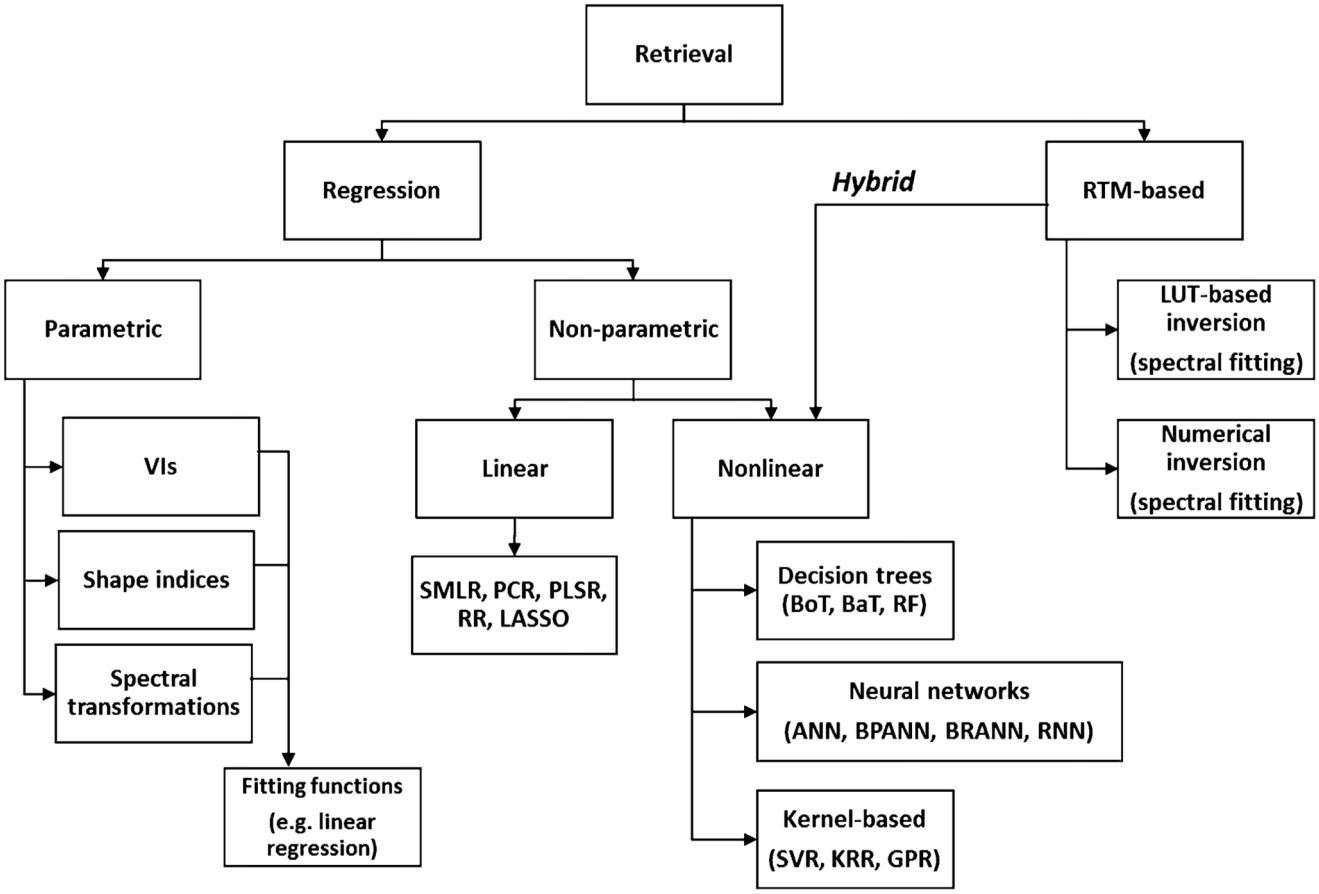

Figure 9. Schematic overview of the main retrieval methods

Europe PMC Funders Author Manuscripts

Europe PMC Funders Author Manuscripts

Table 1

Linear nonparametric regression methods applicable to spectroscopic data

Method	Description	References
Stepwise multiple linear regression (SMLR)	SMLR recursively applies multiple regression a number of times. Each step removes a variable eliciting the weakest correlation. At the end of the recursive process, a variable set is obtained that is optimally explaining the spectral data distribution	Draper and Smith (2014)
Principal components regression (PCR)	PCR is a regression analysis method based on principal components analysis (PCA) estimating regression coefficients. Solutions from PCR are generated performing linear regression of the most relevant components (called scores) obtained after applying PCA	Wold et al. (1987)
Partial least squares regression (PLSR)	PLSR is similar to PSR but tackles the co-linearity problem differently than PCR. Applying PCR, regression is performed using PCA scores. These projections are obtained using only input patterns, not outputs. In contrast, PLSR builds the regression model on projections obtained using the partial least squares (PLS) approach. It elicits the directions of maximum input–output cross-covariance. Therefore, PLSR takes both input patterns and output variables into account	Geladi and Kowalski (1986)
Ridge (regulated) regression (RR)	RR is the most commonly used method of regularization for ill-posed problems, which are problems that do not have a unique solution. RR deals with co-linearity by allowing a degree of bias in the estimates. Therefore, RR adds a small positive value λ to the diagonal elements of the input data covariance matrix. Hence, RR requires finding an optimal value for λ. Typically, cross-validation is used to reach near optimal values. An important fact about RR is that it enforces the regression coefficients to be lower, but it does not enforce them to be zero. That is, it will not get rid of irrelevant features (bands) but rather minimize their impact on the trained model	Geladi and Kowalski (1986)
Least absolute shrinkage and selection operator (LASSO)	Lasso is a extension built on RR, but with a small twist. It also penalizes the regression coefficients absolute size. By this penalization some of the variable estimates may be exactly zero. The larger the penalty, the more the estimates will tend towards zero. This is a convenient approach to automatically perform feature selection, or to deal with correlated predictors	Tibshirani (1996)

Europe PMC Funders Author Manuscripts

Table 2

Decision tree regression methods applicable to spectroscopic data

Method	Description	References
Decision trees (DT)	DT learning is based on decision tree predictive modelling. A decision tree is based on a set of hierarchical connected nodes. Each node represents a linear decision based on a specific input feature	Breiman et al. (1984)
Boosted trees (BoT)	BoT incrementally builds an ensemble by training each new instance to emphasize the training instances previously mis-modelled	Friedman et al. (2000)
Bagging trees (BaT)	BaT is an early ensemble method based on building multiple decision trees by iteratively replacing resampled training data and voting for the decision trees leading to a consensus prediction	Breiman (1996)
Random forest (RF)	RF is a specific type of BaT that in constructs a collection of decision trees with controlled variance	Breiman (2001)

Europe PMC Funders Author Manuscripts

Table 3

Artificial neural network regression methods applicable to spectroscopic data

Method	Description	References
Artificial neural networks (ANNs)	ANNs in their basic form are essentially fully connected layered structures of artificial neurons (AN). An AN is basically a pointwise nonlinear function (e.g., a sigmoid or Gaussian function) applied to the output of a linear regression. ANs with different neural layers are inter-connected with weighted links. The most common ANN structure is a feedforward ANN, where information flows in a unidirectional forward mode. From the input nodes, data pass hidden nodes (if any) towards the output nodes	Haykin (1999)
Back-propagation ANN (BPANN)	The basic type of neural network is multi-layer perceptron, which is feedforward back-propagation ANN. BPANN consists of 2 steps: (1) feedforward the values and (2) calculate the error and propagate it back to the earlier layers. So to be precise, forward-propagation is part of the back-propagation algorithm but comes before back-propagating. This is the most commonly used algorithm when referring to ANN. In many papers using ANN, these standard designs are not explicitly mentioned	Haykin (1999)
Radial basis function ANN (RBFANN)	RBFANN is a type of ANN that uses nonlinear radial basis functions (RBFs) as activation functions in the hidden layer. The output of the network is a linear combination of RBFs of the inputs and neuron parameters	Broomhead and Lowe (1988)
Recurrent ANN (RANN)	A RANN is a type of ANN that make use of sequential information by introducing loops in the network	Hochreiter and Schmidhuber (1997)
Bayesian regularized ANN (BRANN)	BRANNs are more robust than standard BPANNs and can reduce or eliminate the need for lengthy cross-validation. Bayesian regularization is a mathematical process that converts a nonlinear regression into a “well-posed” statistical problem in the manner of a ridge regression	Burden and Winkler (1999)

Europe PMC Funders Author Manuscripts

Table 4

Kernel-based regression methods applicable to spectroscopic data

Method	Description	References
Support vector regression (SVR)	The support vector machine (SVM) is a supervised machine learning technique that was invented in the context of the statistical learning theory. It was not until the mid-1990s that an algorithm implementation of the SVM was proposed with the introduction of the kernel trick and the generalization to the non-separable case. SVR is built on the principle of SVM: a nonlinear function is learned by linear learning machine mapping into high-dimensional kernel induced feature space. The capacity of the system is controlled by parameters that do not depend on the dimensionality of feature (bands) space	Vapnik et al. (1997)
Kernel ridge regression (KRR)	KRR combines RR with the kernel trick. It thus learns a linear function in the space induced by the respective kernel and the data. For nonlinear kernels, this corresponds to a nonlinear function in the original space. The form of the model learned by KR is identical to SVR. However, different loss functions are used: KRR uses squared error loss, while SVR uses ϵ-insensitive loss combined with RR regularization	Suykens and Vandewalle (1999)
Gaussian process regression (GPR)	GPR is based on Gaussian processes (GPs), which generalize Gaussian probability distributions in a function's space. A GP is stochastic since it describes the properties of functions. As in Gaussian distributions, a GP is described by its mean (which for GPs is a function) and covariance (a kernel function). This represents an expected covariance between function values at a given point. Because a GPR model is probabilistic, it is possible to compute the prediction intervals using the trained model	Rasmussen and Williams (2006)

Table 5
Advanced canopy RTMs commonly used in imaging spectroscopy applications

RTM	Description
SCOPE(Soil–Canopy–Observation of Photosynthesis and Energy fluxes)	SCOPE (Tol et al. 2009) is a soil–vegetation–atmosphere (SVAT) scheme that includes RTMs along with a micrometeorological model for simulating turbulent heat exchange, and a plant physiological model for photosynthesis (Tol et al. 2014). The radiative transfer scheme is based on SAIL (Verhoef 1984b, 1985), extended with a similar radiative transfer for emitted radiation. The emitted radiation includes chlorophyll fluorescence and thermal radiation. Leaf radiative transfer is calculated with Fluspect (Vilfan et al. 2016) which also includes emitted fluorescence radiation. SCOPE is intended as tool to scale processes from leaf to canopy, and to analyse the effects of light scattering. Recent developments include vertical heterogeneity (Yang et al. 2017) and the zeaxanthin–violaxanthin pigment cycles
Discrete Anisotropic Radiative Transfer (DART)	DART model is being developed since 1992 as a physically based 3D computer programme (Gastellu-Etchegorry et al. 1996), which simulates radiative budget and remote sensing (airborne and spaceborne) optical image data of natural and urban landscapes for any wavelengths from the ultraviolet to the thermal infrared part of the electromagnetic spectrum (Gastellu-Etchegorry et al. 1999; Guillevic et al. 2003). It computes and provides bottom and top of the atmosphere spectral quantities (i.e. irradiance, exitance and radiance) that are transformed into reflectance or brightness temperature depending on the user DART mode preferences (Gastellu-Etchegorry et al. 2004). Simulated scenes may include the atmosphere, topography and any natural or anthropogenic objects at any geographical location (Grau and Gastellu-Etchegorry 2013). The latest DART optical development includes also the specular reflectance and the light polarization (Gastellu-Etchegorry et al. 2015). Apart of passive remote sensing data, it also simulates active terrestrial and air-/spaceborne light detection and ranging (LiDAR) discrete return, full waveform, multi-pulse and photon counting measurements (Gastellu-Etchegorry et al. 2016; Yin et al. 2016). In case of vegetation, it can also simulate radiative transfer of the solar-induced chlorophyll fluorescence for any virtual 3D Earth scene numerically and as images (Gastellu-Etchegorry et al. 2017)
Librat	Librat is a 3D Monte Carlo ray-tracing radiative transfer model developed as a library interface to the original ararat (Advanced RAdiometric RAy Tracer) model. The first version of ARARAT was published in 1992 (Lewis and Muller 1993) as part of the Botanical Plant Modelling System (BPMS) (Lewis 1999; Lewis and Muller 1990). Subsequently, the sampling scheme was improved as reported in Saich et al. (2002), and the codes developed into a library in recent years. Librat reads a 3D description of (canopy/soil/topographic) geometry, along with associated information on material scattering properties. The main function in the library then is that a ray is launched from some origin in 3D space, in a specified direction, and the code returns all information about the associated scattering paths and interactions, separated as direct and diffuse components. This core functionality, along with a set of associated sensor models but integrating paths, fired into some volume. It allows for a wide range of radiative transfer calculations, including time-resolved/lidar, splitting of the radiometric information per scattering order as well as straightforward reflectance/transmittance calculations (e.g., Disney et al. 2006; Hancock et al. 2012)
FLIGHT	FLIGHT (Barton and North 2001; North 1996) is a Monte Carlo ray-tracing model designed to rapidly simulate light interaction with 3D vegetation canopies at high spectral resolution, and produce reflectance spectra for both forward simulation and for use in inversion (Leonenko et al. 2013). Foliage is represented by structural properties of leaf area, leaf angle distribution, crown dimensions and fractional cover, and the optical properties of leaves, branch, shoot and ground components. The model represents multiple scattering and absorption of light within the canopy and with the ground surface. It has been developed to model 3D canopy photosynthesis (Alton et al. 2007), to simulate waveform and photon counting lidar (Montesano et al. 2015; North et al. 2010) and emitted fluorescence radiation (Hernández-Clemente et al. 2017). Structural data may be specified as a statistical distribution, derived from field measurements (Morton et al. 2014) or by direct inversion from LiDAR data (Bye et al. 2017)